GEOLOGICA SAXONICA
Journal of Central European Geology

59: 45–63
12 Sept 2013

SENCKENBERG

U-Pb ages of detrital zircons, fossils, and facies of the Cambro-Ordovician overstep sequence of the eastern Lausitz Block (Dubrau and Ober-Prauske formations, Saxo-Thuringian Zone)

U-Pb-Alter detritischer Zirkone, Fossilien und Fazies der kambro-ordovizischen Sedimentabfolge des östlichen Lausitz-Blocks (Dubrau- und Ober-Prauske-Formation, Saxothuringische Zone)

Claudia Franz [1], Ulf Linnemann [2], Mandy Hofmann [2], Ronald Winkler [3] and Bernd Ullrich [4]

[1] Technische Universität Dresden, Institut für Geographie, Helmholtzstraße 10, 01069 Dresden, Germany; claudia.franz@tu-dresden.de — [2] Senckenberg Naturhistorische Sammlungen Dresden, Museum für Mineralogie und Geologie, Sektion Geochronologie, Königsbrücker Landstraße 159, 01109 Dresden, Germany — [3] Senckenberg Naturhistorische Sammlungen Dresden, Museum für Mineralogie und Geologie, Sektion Paläozoologie, Königsbrücker Landstraße 159, 01109 Dresden, Germany — [4] Technische Universität Dresden, Institut für Geotechnik, George-Bähr-Straße 1, 01069 Dresden, Germany

Revision accepted 19 June 2013.
Published online at www.senckenberg.de/geologica-saxonica on 10 September 2013.

Abstract

The Cadomian basement of the eastern Lausitz Block is transgressed by the Ober-Prauske Formation (Cambrian, undifferentiated) and the Dubrau Formation (Tremadocian, Lower Ordovician). Both formations are remnants of the Early Palaeozoic overstep sequence, which overlies unconformable the Cadomian basement. The Ober-Prauske Formation consists of shallow marine red sandstones. Fossils are unknown. The age of sedimentation for the red sandstones is bracketed between ~ 542 Ma (youngest zircon) and the overlying Dubrau Formation (Tremadocian). The latter one is a shallow marine sedimentary succession of high mature siliciclastics. The depositional setting of the fossil-rich Dubrau Formation was a shallow marine shelf of an open sea or ocean and not a protected environment. The section starts with a basal conglomerate containing an association of stable clasts like tourmaline hornfels, vein quartz, quartzite, and silicified sandstone. The identification of the *Skolithos* and *Cruziana* ichnofacies characterize the middle part of the Dubrau Formation as deposits of the middle to lower shoreface. Both, the *Skolithos* and *Cruziana* ichnofacies, grade into strata characterized by frequent hummocky cross-stratification and a total lack of macrofossils, which are upper to lower offshore deposits. Most Cambrian strata are missing in the section. That gap in sedimentation may have been originated by the rift and drift-off of Avalonia or a related terrane and a consequent doming of the astenosphere. The latter one caused strong chemical weathering, erosion, and a gap in the most of Cambrian time. Thermal subsidence at the beginning of the Ordovician controlled the new onset of deposition. The high maturity of the sedimentary rocks of the Dubrau Formation and a lot of other Lower Ordovician sediments in the Saxo-Thuringian Zone was originated by strong chemical weathering in the source area in Middle–Upper Cambrian time. At the base of U-Pb dating of the detrital zircon grains from the Ober-Prauske and Dubrau formations a derivation of the clastic debris from the West African Craton is concluded. Little input of Mesoproterozoic zircon grains in the Ober-Prauske Formation was derived from Amazonia. Sedimentary rocks of the Ober-Prauske and Dubrau formations were formed in the framework of peri-Gondwana. During the formation of Pangaea and the related origin of the Variscan Orogen, the peri-Gondwanan Lausitz Block including its overstep sequence was incorporated into the Central European Variscides.

ISBN 978-3-910006-37-9 | ISSN 1617-8467

Kurzfassung

Das Cadomische Grundgebirge des östlichen Lausitz-Blocks wird von der kambrischen Ober-Prauske-Formation und der unterordovizischen Dubrau-Formation (Tremadocium) transgressiv überlagert. Beide Formationen stellen reliktische Vorkommen einer einstmals flächenhaft verbreiteten Überlappungssequenz dar. Die Ober-Prauske-Formation besteht aus roten Sandsteinen, die im flachmarinen Milieu abgelagert wurde. Das Alter dieser Formation liegt zwischen ~ 542 Ma (jüngster Zirkon) und dem Tremadocium der auflagernden Dubrau-Formation. Letztere stellt eine flachmarine sedimentäre Abfolge hochmaturer siliziklastischer Sedimentgesteine dar. Das Ablagerungsmilieu der fossilreichen Dubrau-Formation war ein flachmariner Schelf einer offenen See oder Ozeans. Die Formation beginnt mit einem Basiskonglomerat, das aus Stabilkomponenten-Geröllen wie Turmalinhornfels, Gangquarz, Quarzit und verkieseltem Sandstein besteht. *Skolithos*- und *Cruziana*-Ichnofazies charakterisieren den mittleren Teil der Dubrau-Formation als Ablagerungen des mittleren bis unteren Vorstrandes. Diese Ablagerungen gehen im Hangenden in ein Schichtglied über, dass durch Sturmablagerungen (Tempestite) mit hügeliger Schrägschichtung (HCS) und ein totales Fehlen von Makrofossilien ausgezeichnet ist. Diese Sedimentgesteine repräsentieren Ablagerungen des oberen bis unteren Offshore-Bereichs. In der kambro-ordovizischen Gesamtabfolge fehlt der größte Teil des Kambriums. Diese Sedimentationslücke wird mit der Riftbildung und dem Wegdriften von Avalonia oder einem verwandten Terrane sowie der damit verbundenen Aufdomung der Astenosphäre erklärt. Letztere erzeugte ein Trockenfallen, chemische Verwitterung, Erosion und eine Schichtlücke, die fast das gesamte Kambrium umfasst. Thermale Subsidenz kontrollierte das Einsetzten der unterordovizischen Sedimentation. Die hohe Reinheit der ordovizischen Quarzite in der Saxothuringischen Zone ist einer tiefgründigen Verwitterung im mittleren bis oberen Kambrium zuzuschreiben. Auf der Basis der U-Pb-Alter detritischer Zirkone aus den Sandsteinen der Ober-Prauske- und Dubrau-Formation wird die Herkunft dieser Sedimentgesteine vom Westafrikanischen Kraton abgeleitet. Ein geringer Anteil der Zirkone aus der Ober-Prauske-Formation stammt aus Amazonia (nördliches Südamerika). Die Ober-Prauske- und die Dubrau-Formation sind typische Ablagerungen peri-Gondwanas. Während der Pangäa-Bildung und der damit einhergehenden variszischen Orogenese wurde der Lausitz-Block einschließlich seiner kambro-ordovizischen Auflagerung in die mitteleuropäischen Varisziden eingebaut.

1. Introduction

The Ober-Prauske and Dubrau formations form a section of Cambro-Ordovician siliciclastic sediments, which occurs in the eastern Lausitz Block of the Saxo-Thuringian Zone. The latter one is an important geotectonic unit in the framework of the Bohemian Massif, which is one of the most dominant crustal units of the Central European Variscides (Fig. 1). The Ober-Prauske Formation consists of spot-like occurrences of red sandstones. The type locality is represented by remnants of an old quarry in a small forest near the village of Ober-Prauske. Due to the results of geological mapping and the field situation (Lee 1938) the Ober-Prauske Formation overlies the Neoproterozoic to Fortunian greywackes (~ 542 Ma) of the Lausitz Group and is overstepped by the white and high mature quartzites of the Dubrau Formation. The depositional age of the Ober-Prauske Formation is bracketed between the c. 542 Ma old underlying Lausitz Group (Linnemann et al. 2007) and the overlying Dubrau Formation (Tremadocian, c. 485 Ma). As a consequence, the Ober-Prauske Formation is Cambrian in age. Due to the lack of fossils a more detailed classification concerning its age is not possible. The sedimentary sequence of the younger Dubrau Formation is restricted to a quite small area of a few square kilometres near the village of Groß-Radisch in the eastern Lausitz (Fig. 2). The siliciclastics of the Dubrau Formation are represented by high mature conglomerates, microconglomerates, quartzites, and minor shales. The unusual rich occurrence of trace fossils, the low metamorphic overprint (lower greenschist facies), and the very weak tectonic deformation style (one less evolved cleavage) is very unique for the Saxo-Thuringian Zone. Further, it is the only Ordovician sedimentary sequence, which overlies the Cadomian basement of the Lausitz Block (Linnemann & Buschmann 1995). Other Ordovician occurrences (e.g., Eichberg Formation) are olistoliths in a Lower Carboniferous wildflysch succession of the Görlitz Schist Belt (Görlitzer Schiefergebirge; Linnemann et al. 2010), which is an adjoining geotectonic unit to the northeast of the Lausitz Block (Fig. 1). The Dubrau Formation provides important information of a Lower Ordovician faunal assemblage in a shallow water regime of high latitudes on the southern hemisphere. Further, sedimentary rocks can deliver very useful information concerning environmental conditions, provenance of sedimentary rocks, and palaeogeography. Concerning these special features, the Dubrau Formation was underestimated for a long time. In that paper, we try to close a gap of important geological information. We present details on sedimentary facies, the fossil assemblage, and U-Pb ages of detrital zircons. The latter ones are interpreted in view of provenance of sediments and the palaeogeographical position during the time of origin of the Dubrau Formation.

2. Geological setting

The main distribution of the red sandstones of the Ober-Prauske Formation is located in the remnants of the old quarry near Ober-Prauske, which is situated in a little forest. The coordinates are given in the heading of Tab. 1. On the agricultural fields situated in the closer surrounding of that forest spot the red sandstone also occurs as loose blocks. Outcrop situation is really bad. On the hand specimens sometimes primary sedimentary structures like low-angle cross-stratification occur, which points to shallow marine nature for the red sandstone units. The

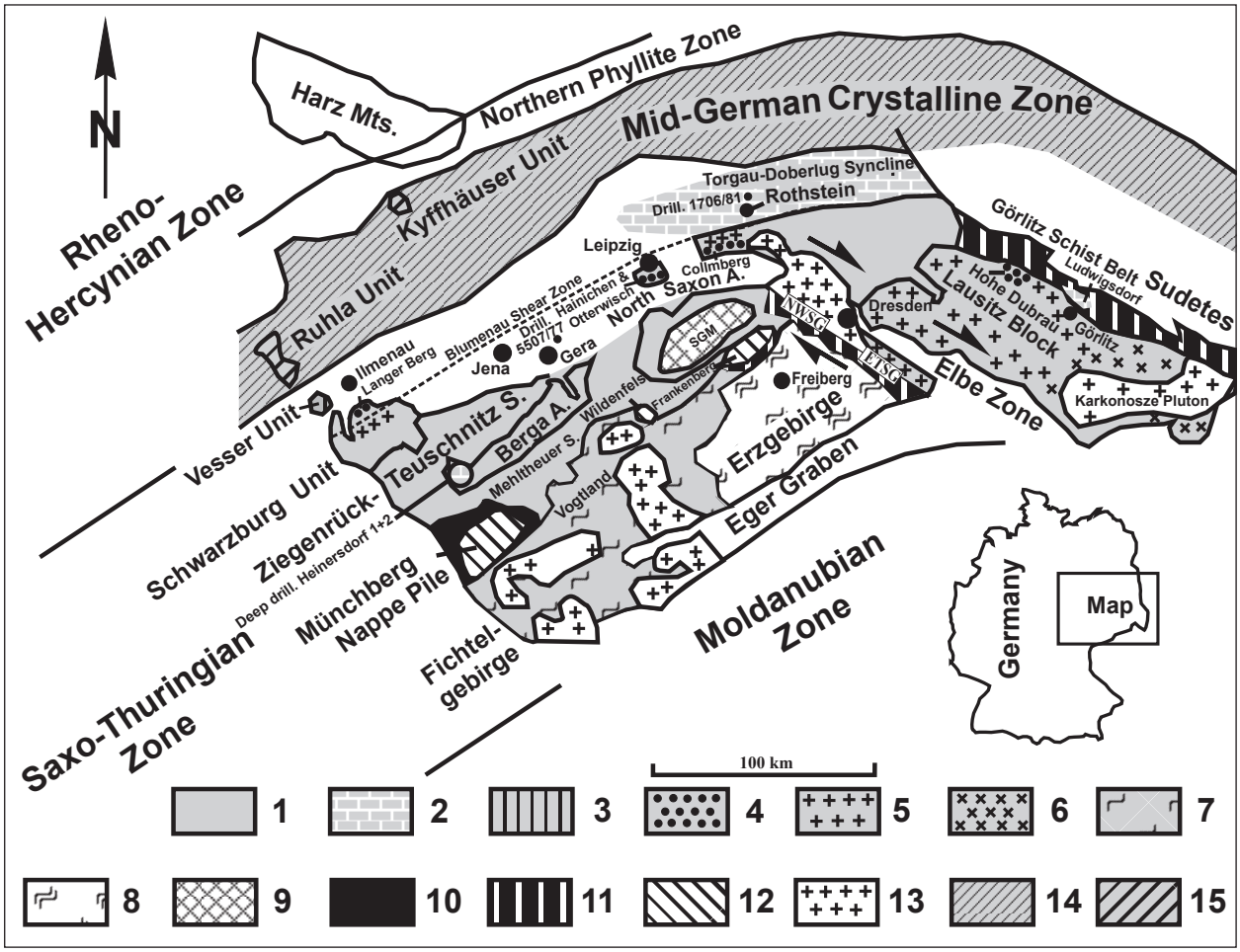

Fig. 1. Simplified geological map of the Saxo-Thuringian Zone showing the distribution of Palaeozoic sedimentary rocks of the Thuringian and the Bavarian Facies (modified after Linnemann et al. 2000, 2010). **NWSG**, Nossen-Wilsdruff Schist Belt; **ETSG**, Elbtal Schist Belt (both are parts of the schist belt of the Elbe Zone). **1**, General distribution of Cadomian basement and overlying Palaeozoic sedimentary rocks of the Thuringian Facies; **2**, Lower to Middle Cambrian of the Thuringian Facies; **3**, Middle to Upper Cambrian rocks of the Vesser Unit; **4**, External segment of the Saxo-Thuringian Zone where Ordovician rocks are present only as very thick, bedded, and highly mature Tremadocian quartzites; **5**, Cadomian plutons (~ 540 Ma); **6**, Lower Ordovician plutons (~ 490 Ma); **7**, Metamorphosed Palaeozoic rocks of the Thuringian Facies (phyllites and garnet phyllites of the mid-pressure/low-temperature and the low-pressure/low-temperature units of the nappe pile of the Erzgebirge and adjoining areas); **8**, Mid-pressure/mid-temperature metamorphosed Cadomian basement rocks of the Freiberg and Reizenhain gneiss domes and Palaeozoic rocks of the and the high-pressure/high-temperature nappes of the Erzgebirge; **9**, High grade metamorphosed rocks of the Saxonian Granulite Massif; **10**, Palaeozoic sedimentary rocks of the Bavarian Facies; **11**, Palaeozoic sedimentary rocks with mixed distribution of Thuringian and Bavarian Facies; **12**, High grade metamorphic rocks of the nappes of the Münchberg Nappe Pile and the Zwischengebirge of Wildenfels and Frankenberg; **13**, Variscan granites (~ 335 – 325 Ma); **14**, Metamorphic rocks of the Mid-German Crystalline Zone (covered by post-Variscan strata); **15**, Metamorphic rocks of the Mid-German Crystalline Zone (outcrop).

Abb. 1. Vereinfachte geologische Karte der Saxothuringischen Zone mit der Verbreitung des Paläozoikums in Thüringischer und Bayerischer Fazies.

deposits are comparable to the initial red beds of the Cambro-Ordovician in Brittany (Armorican Massif).

The Dubrau Formation is situated in the surrounding fields and forests close to the village of Groß-Radisch, especially in the areas of the Hohe Dubrau, the Kollmer Dubrau, the Kreutzschenker Höhe, and the Monumentenberg (Fig. 2). The sedimentary rocks of the Dubrau Formation (formerly Dubrau Quarzit) are first described by Cheng-San Lee (1938) and Hirschmann (1960 cited in Pietzsch 1962). Later geological descriptions (e.g., Brause 1969) referred to the Dubrau Quarzit, but yielded no significant new results. After a period of long "scientific silence" concerning the geology of the Dubrau Formation, Linnemann & Buschmann (1995) described for the first time the Cadomian unconformity from the Saxo-Thuringian Zone and placed the type area in the Hohe Dubrau and at the Monumentenberg. Due to new mapping and measurement of sections it became clear, that the Dubrau Formation overlies discordant the folded and deformed greywackes of the Lausitz Group, which are latest Neoproterozoic to earliest Cambrian in age (Linnemann et al. 2007). Further, Linnemann & Buschmann (1995) could characterize the Dubrau Formation as a Lower Ordovician marine overstep sequence starting

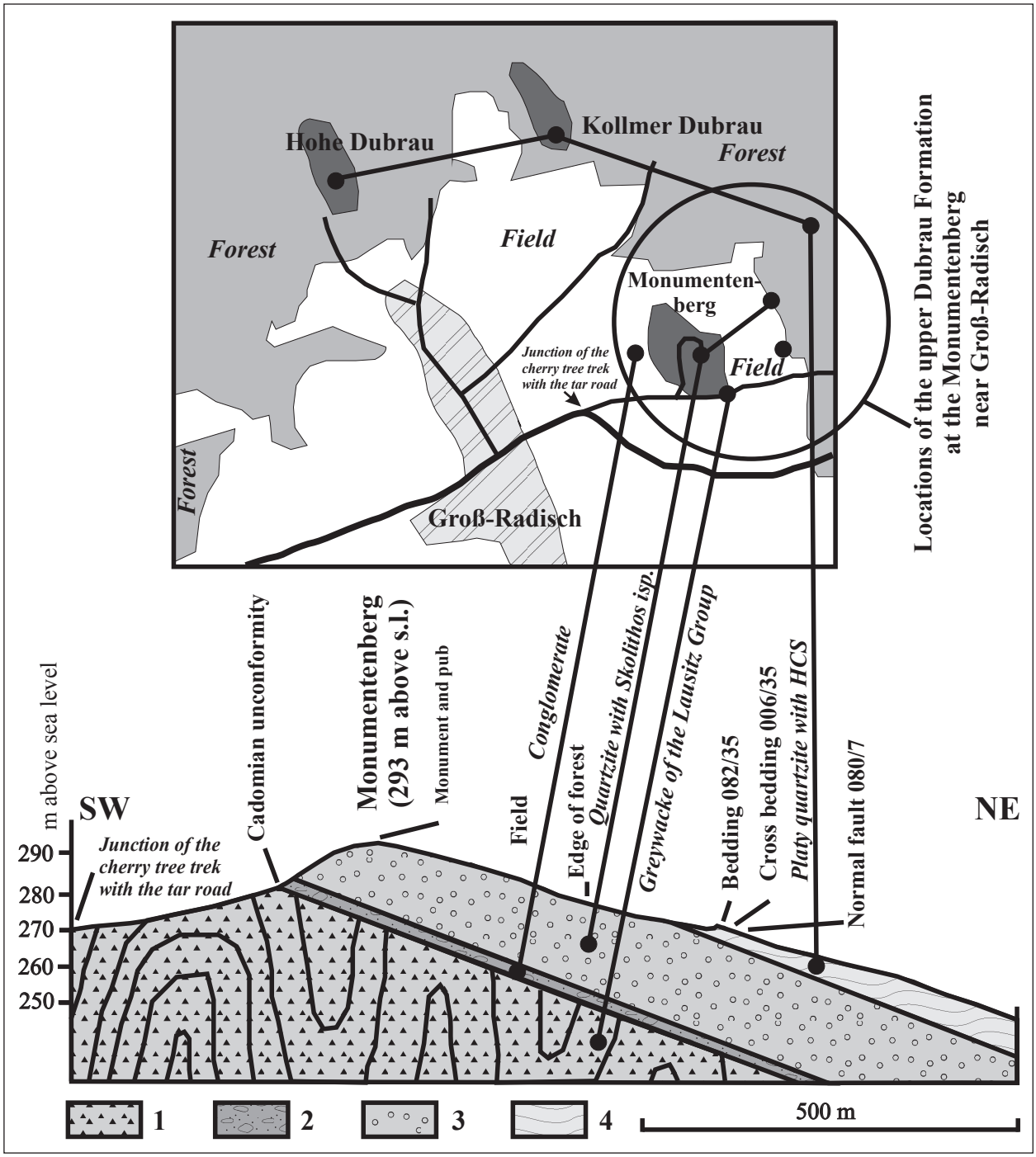

Fig. 2. Locations and cross section of the Dubrau Formation (Tremadocian, Lower Ordovician; after Linnemann & Buschmann 1995): **1**, Greywacke; **2**, Basal conglomerate; **3**, Quartzite with *Skolithos* isp.; **4**, Quartzite with HCS.

Abb. 2. Vorkommen und Profil der Dubrau-Formation (Tremadocium, Unteres Ordovizium).

with a basal conglomerate (Fig. 3a, b), which is overlain by a thin- to thick-bedded quartzite with lots of *Skolithos* tubes (Fig. 3c) and fragments of brachiopod shells. Microconglomeratic levels are frequent in the strata with the trace fossil *Skolithos*. Beds with *Skolithos* isp. often show a microconglomerate at the base, which grades into sandstone or quartzite, respectively. The basal conglomerate and the strata of microconglomerates consist of clasts of vein quartz, sandstones, and fragments of tourmaline hornfels. In large fragments of the tourmaline hornfels brecciated fragments of quartzite can be observed (Fig. 3a, b). The origin of the fragmented hornfels most probably is related to contact metamorphism related to the intense plutonism in the Lausitz Block at c. 540 Ma, which was part of the final pulse of the Cadomian orogeny (Linnemann et al. 2000). First findings of *Cruziana* isp. in the *Skolithos*-bearing strata were described by Linnemann (2003). The upper part of the Dubrau Formation is represented by thin-bedded quartzites showing features of a storm-dominated depositional regime,

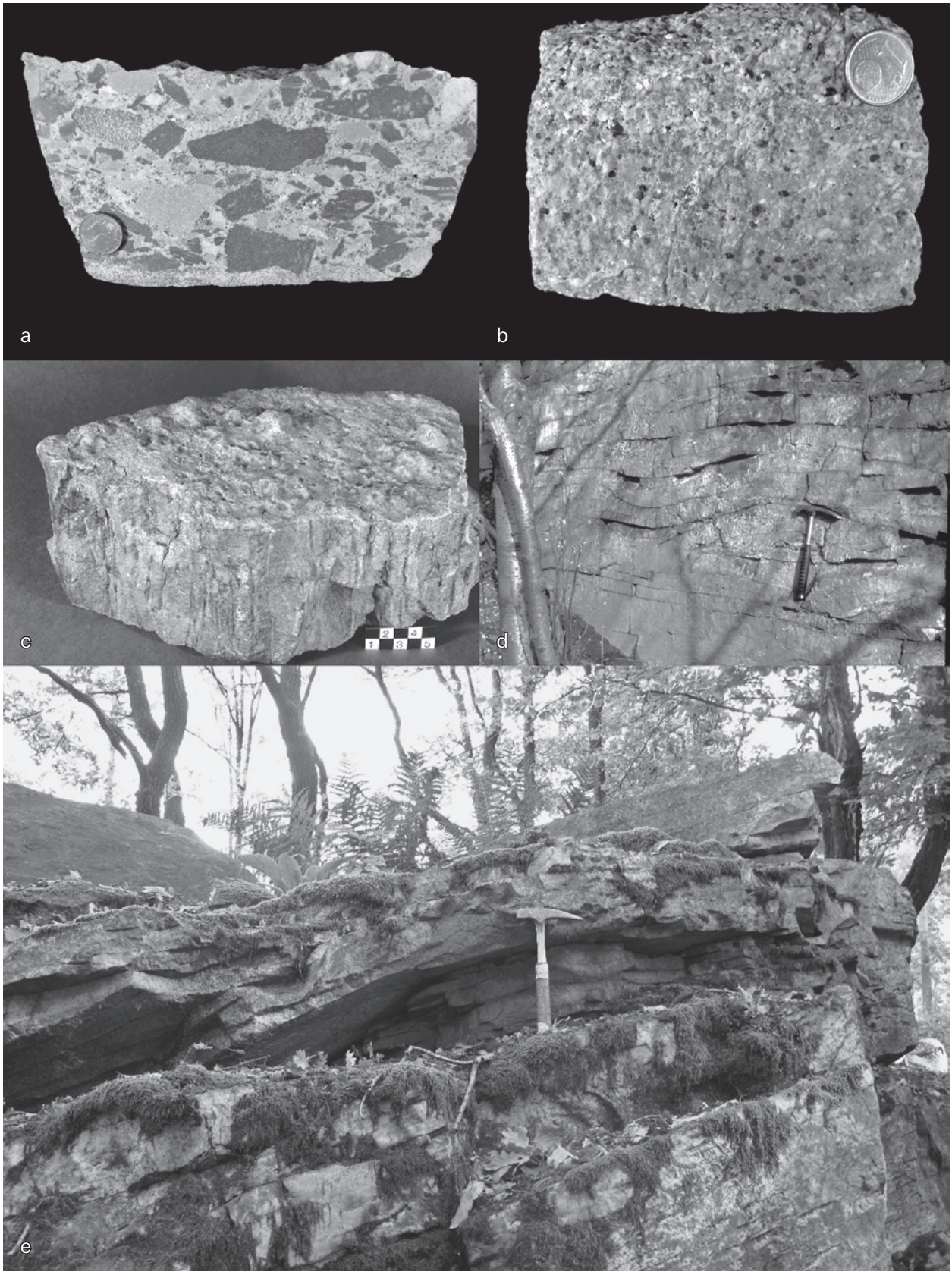

Fig. 3. Sedimentary rocks of the Dubrau Formation: **a**, Matrix-supported conglomerate with fragments of tourmaline hornfels, sandstones, and vein quartz from the base of the Dubrau Formation (Monumentenberg); **b**, Micro-conglomerate with sub- to well-rounded clasts of vein quartz, quartzite, sandstone, and tourmaline hornfels (Monumentenberg); **c**, Quartzite bed with *Skolithos* isp. from the middle part of the Dubrau Formation (Monumentenberg); **d**, Hummocky cross-stratification (HCS) in the upper part of the Dubrau Formation (Hohe Dubrau); **e**, Out-weathered HCS in the upper part of the Dubrau Formation (northeast of the Monumentenberg).

Abb. 3. Sedimentgesteine der Dubrau-Formation.

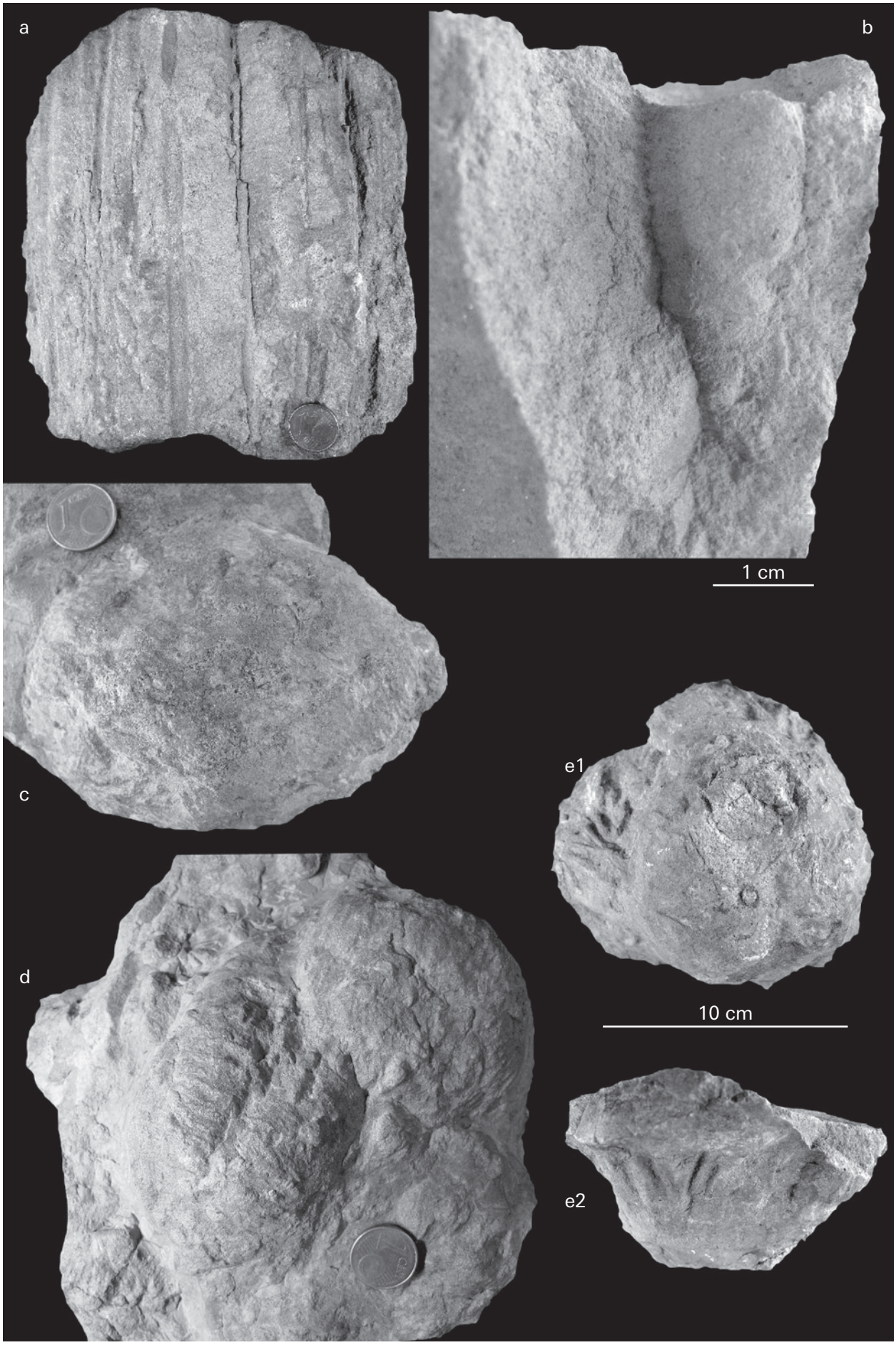
a
b
1 cm
c
e1
10 cm
d
e2

like hummocky cross-stratification (HCS; Fig. 3d, e) and the lack of any macrofossils. According to the mapping results of Linnemann & Buschmann (1995) the entire section of the Dubrau Formation is about 150 m thick. Younger strata are not preserved in the area. Outcrops are scarce. Often the rocks can be studied at the edges of the fields. The location of significant outcrops is shown in Fig. 2.

3. Fossil assemblage, sedimentary facies, stratigraphy

Systematic collecting of fossils over a number of years by staff members of the Senckenberg Naturhistorische Sammlungen Dresden, Museum of Mineralogy and Geology, resulted in a representative overview of taxa, which occur in the Dubrau Formation. The fossil assemblage found so far consists of a trace fossil community (Fig. 4) and shells of brachiopods (Fig. 5). Among the trace fossils, *Skolithos* isp. is very frequent in the middle part of the section. Tubes are between c. 3 cm and 15 cm long and show a diameter of c. 3 mm (Fig. 4a). Traces of coelenterate resting burrows (*Bergaueria* isp.) occur, but are scarce (Fig. 4b). Different types of resting traces of trilobites (*Cruziana* isp.) are very scarce as well (Fig. 4c, d, e1, e2). Body fossils of trilobites or parts of it never have been found.

The known trace fossils are not good enough as stratigraphical key fossils. Instead, they are very good facies indicators (Crimes 1975, Frey & Seilacher 1980, Seilacher 2007). In the Dubrau Formation, the *Skolithos* ichnofacies grades into the *Cruziana* ichnofacies. The latter one is overlain by fossil-free beds with hummocky cross-stratification (HCS). That succession points to a deepening-upward trend and characterizes the Dubrau Formation as a part of a transgressive systems tract (TST) in terms of sequence stratigraphy (van Wagoner et al. 1990).

The *Skolithos* ichnofacies is indicative of relatively high levels of wave or current energy, and typically is developed in clean, well-sorted, loose or shifting particulate substrates. Abrupt changes in rates of deposition, erosion, and physical reworking of sediments are frequent. The *Skolithos* ichnofacies grades landward into supratidal or terrestrial zones and seaward into the *Cruziana* ichnofacies (Pemberton et al. 2001).

In contrast, the *Cruziana* ichnofacies is most characteristic of subtidal, poorly sorted unconsolidated substrates. In deed, in the Dubrau Formation, *Cruziana* isp. could only be identified, when intercalations of dark grey to black shale occurred between two quartzite beds. Conditions of the *Cruziana* ichnofacies range from moderate energy levels in shallow waters, below fair-weather wave base (minimum) but above storm wave base (maximum), to low energy levels in deeper, quieter waters (Pemberton et al. 2001).

According to the shoreface model of Pemberton & MacEachern (1995) the middle part of the Dubrau Formation with *Skolithos* isp. and *Cruziana* isp. represents the middle to lower shoreface. The upper fossil-free part of the formation with frequent HCS is a part of the upper to lower offshore. The depositional setting of the Dubrau Formation was not a protected one like a back barrier or lagoonal setting. Instead, sedimentary environments were characterized by facing to an open sea or ocean.

The occurrence of brachiopods from the Dubrau Formation was described by Geinitz (1873), Schwarzbach (1934, 1936), Kohíla (1937), Lee (1938), Pietzsch (1962), Freyer (1967), Freyer & Wiefel (1991), Heuse & Puura (2000), and Heuse et al. (2010). Brachiopod shells in the Dubrau Formation appear only as isolated shells (Fig. 5a, c), which are enriched sometimes into shell layers (Fig. 5b). The distribution of the brachiopod *Westonisca arachne* Barrande place the Dubrau Formation into the Tremadocian (Heuse & Puura 2000, Heuse et al. 2010).

4. U-Pb LA-ICP-MS dating of detrital zircon

4.1. Methods

Zircon concentrate was separated from 2 kg sample material using standard methods at the Senckenberg Naturhistorische Sammlungen Dresden, Museum für Mineralogie und Geologie, Sektion Geochronologie. Final selection of the zircon grains for U-Pb dating was achieved by hand-picking under a binocular microscope. Zircon grains of all grain sizes and morphological types were selected, mounted in resin blocks, and polished to half their thickness. Zircons were analyzed for U, Th, and Pb

Fig. 4. Trace fossils from the Dubrau Formation (edge of the field of the eastern flank of the Monumentenberg): **a**, The worm tube *Skolithos* isp.; **b**, *Bergaueria* isp., a coelenterate resting burrow; **c**, *Cruziana* isp., a rusophycoid resting trace of a trilobite; **d**, Two individuals of a rusophycoid *Cruziana* isp. on one slab; **e1**, A deep burrowed rusophycoid *Cruziana* isp. (view from the bottom, scale in cm); **e2**, Same specimen as e1 (side view). All specimens are stored in the collection of the Sektion Paläozoologie at the Senckenberg Naturhistorische Sammlungen Dresden, Museum für Mineralogie und Geologie.

Abb. 4. Spurenfossilen aus der Dubrau-Formation (vom Feldrand an der Ostseite des Monumentenberges).

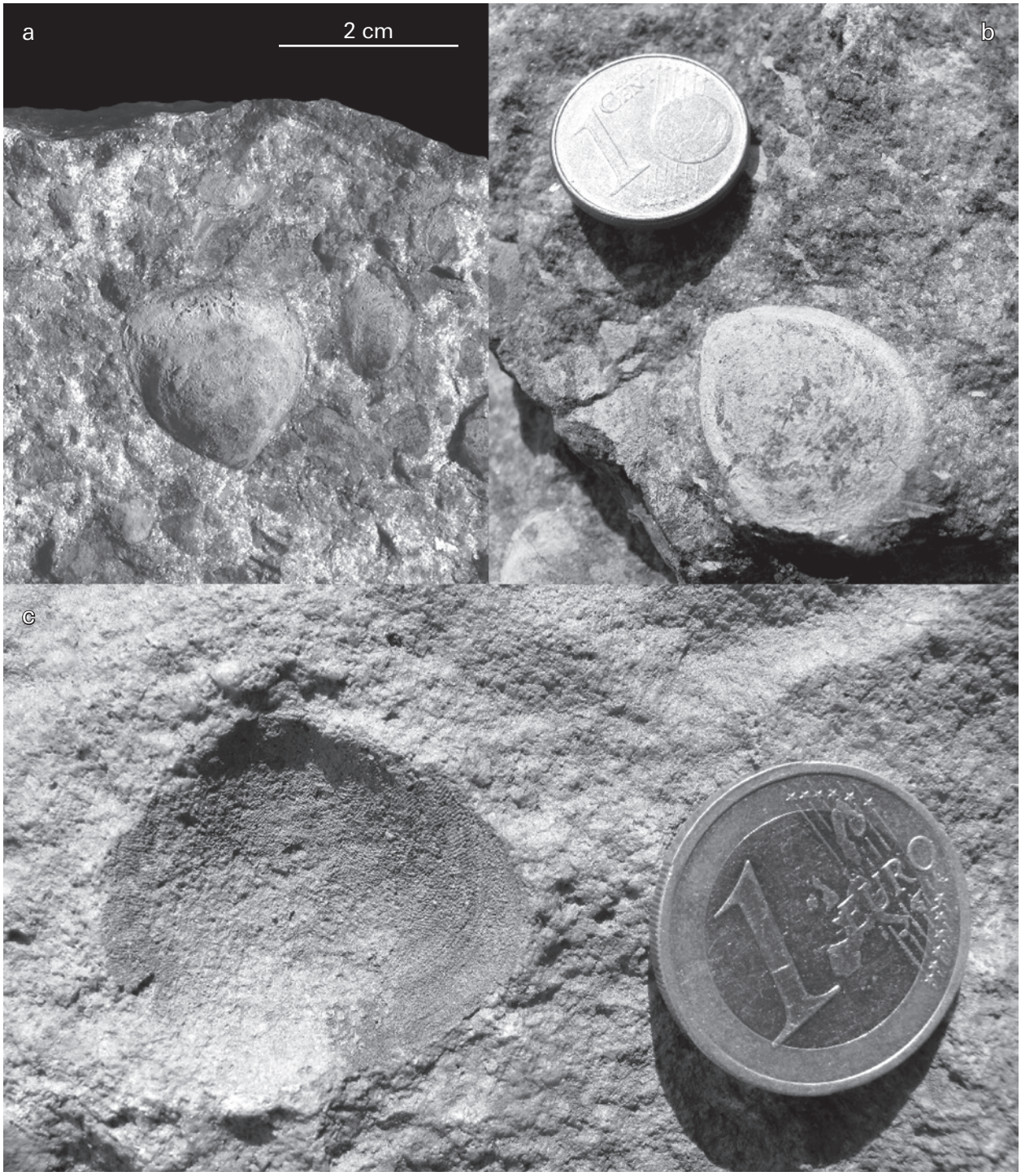

Fig. 5. Brachiopods from the Dubrau Formation (edge of the field of the eastern flank of the Monumentenberg): **a**, *Westonisca arachne* Barrande (Heuse & Puura 2000); **b** and **c**, Diverse brachiopod shells, which could not be determined due to missing diagnostic muscle imprints. All specimens are stored in the collection of the Sektion Paläozoologie at the Senckenberg Naturhistorische Sammlungen Dresden, Museum für Mineralogie und Geologie.

Abb. 5. Brachiopoden aus der Dubrau-Formation (vom Feldrand an der Ostseite des Monumentenberges).

isotopes by LA-ICP-MS techniques, using a Thermo-Scientific Element 2 XR sector field ICP-MS coupled to a New Wave UP-193 Excimer Laser System (Sektion Geochronologie). A teardrop-shaped, low volume laser cell constructed by Ben Jähne (Dresden, Germany) and Axel Gerdes (Frankfurt am Main, Germany) was used to enable sequential sampling of heterogeneous grains (e.g., growth zones) during time resolved data acquisition. Each analysis consisted of approximately 15 s background acquisition followed by 30 s data acquisition, using a laser spot-size of 25 µm and 35 µm, respectively. A common-Pb correction based on the interference- and background-corrected ^{204}Pb signal and a model Pb composition (Stacey & Kramers 1975) was carried out if

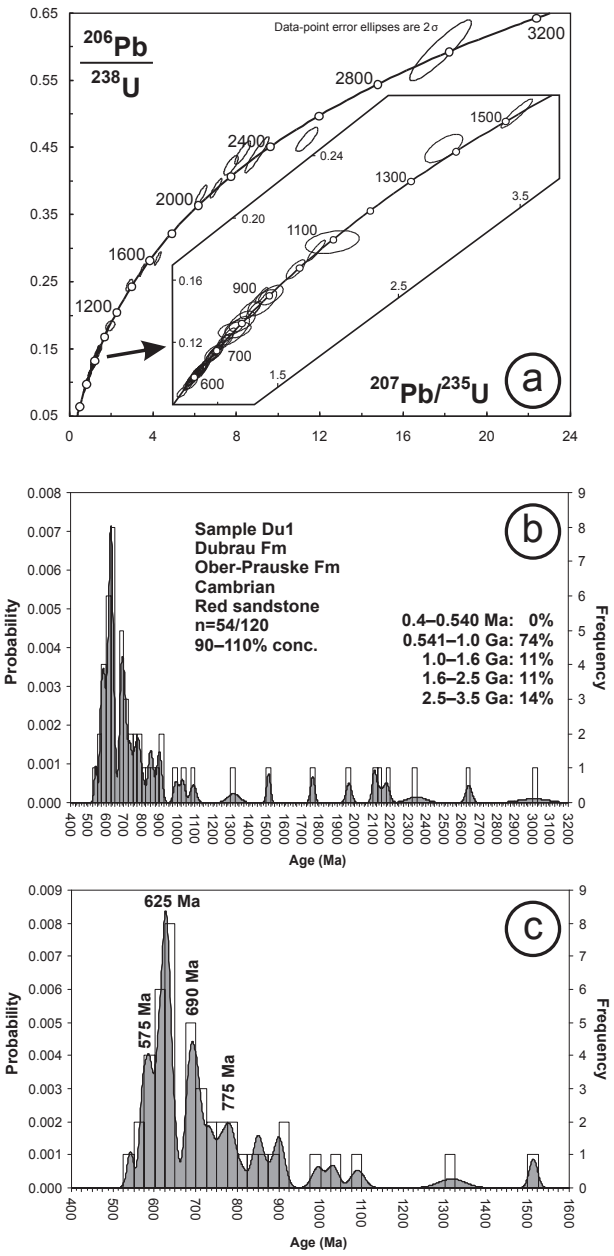

Fig. 6. U-Pb ages of detrital zircon grains from sample Du1 (red sandstone, Ober-Prauske Formation, Cambrian): **a**, Concordia diagram; **b**, Combined binned frequency and probability density distribution plots of detrital zircon grains in the range of 400 – 3500 Ma; **c**, Combined binned frequency and probability density distribution plots of detrital zircon grains in the range of 400 – 1600 Ma.

Abb. 6. U-Pb-Alter detritischer Zirkone der Probe Du1 (roter Sandstein, Ober-Prauske-Formation, Kambrium).

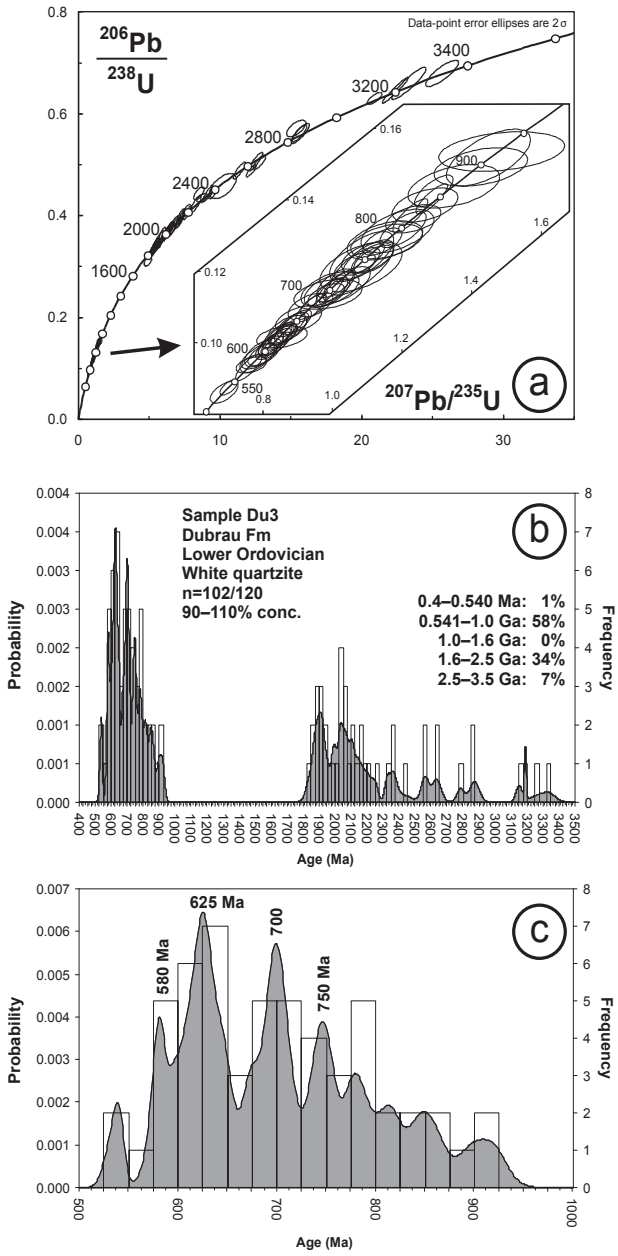

Fig. 7. U-Pb ages of detrital zircon grains from sample Du3 (white quartzite with *Skolithos* isp., Monumentenberg Member, Dubrau Formation, Tremadocian, Lower Ordovician): **a**, Concordia diagram; **b**, Combined binned frequency and probability density distribution plots of detrital zircon grains in the range of 400 – 3500 Ma; **c**, Combined binned frequency and probability density distribution plots of detrital zircon grains in the range of 400 – 1000 Ma.

Abb. 7. U-Pb-Alter detritischer Zirkone der Probe Du3 (weißer Sandstein mit *Skolithos* isp., Monumentenberg-Member, Dubrau-Formation, Tremadocium, Unteres Ordovizium).

necessary. The necessity of the correction is judged on whether the corrected $^{207}Pb/^{206}Pb$ lies outside of the internal errors of the measured ratios. Discordant analyses were generally interpreted with care. Raw data were corrected for background signal, common-Pb, laser induced elemental fractionation, instrumental mass discrimination, and time-dependant elemental fractionation of Pb/Th and Pb/U using an Excel® spreadsheet program developed by Axel Gerdes. Reported uncertainties were propagated by quadratic addition of the external reproducibility obtained from the standard zircon GJ-1 (~ 0.6% and 0.5 – 1% for the $^{207}Pb/^{206}Pb$ and $^{206}Pb/^{238}U$, respectively) during individual analytical sessions and the within-run precision of each analysis. Concordia

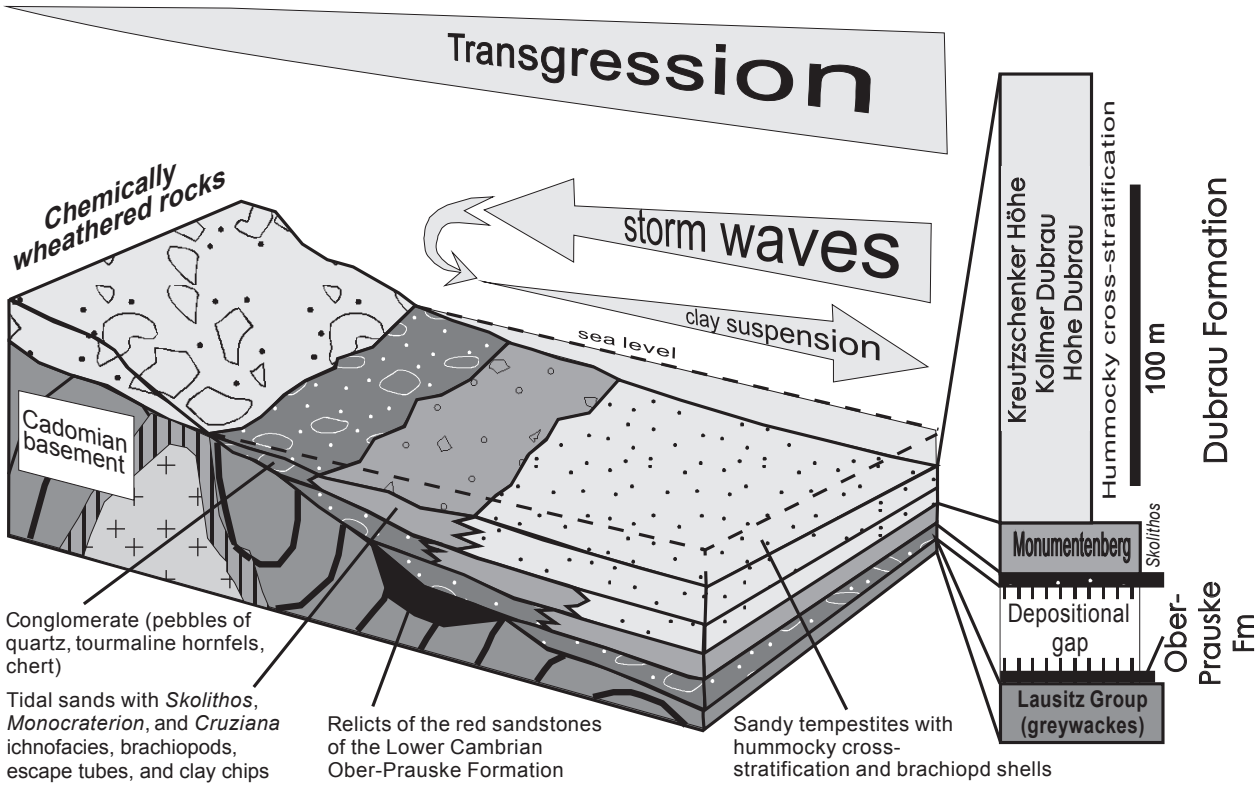

Fig. 8. Reconstruction of the Early Ordovician (Tremadocian) transgression onto the Cadomian basement and the Ober-Prauske Formation (Lower Cambrian) based on the geological mapping at the Monumentenberg and the Hohe Dubrau near Groß-Radisch, Lausitz Block (after Linnemann & Buschmann 1995).

Abb. 8. Rekonstruktion der frühordovizischen Transgression (Tremadocium) auf das cadomische Grundgebirge und die unterkambrische Ober-Prauske-Formation, basierend auf einer geologischen Kartierung am Monumentenberg und in der Hohen Dubrau bei Groß-Radisch, Lausitz-Block (nach Linnemann & Buschmann 1995).

diagrams (2 σ error ellipses) and concordia ages (95% confidence level) were produced using Isoplot/Ex 2.49 (Ludwig 2001), and frequency and relative probability plots using AgeDisplay (Sircombe 2004). The $^{207}Pb/^{206}Pb$ age was taken for interpretation for all zircons > 1.0 Ga, and the $^{206}Pb/^{238}U$ ages for younger grains. Analyses were carried out using the procedures of Gerdes & Zeh (2006) and Frei & Gerdes (2009). For further details on analytical protocol and data processing see that references.

The uncertainty in the degree of concordance of Precambrian–Palaeozoic grains dated by the LA-ICP-MS method is relatively large and results obtained from just a single analysis have to be interpreted with care. A typical uncertainty of 2–3% (2 σ) in $^{207}Pb/^{206}Pb$ for a Late Neoproterozoic grain (e.g., 560 Ma) relates to an absolute error on the $^{207}Pb/^{206}Pb$ age of 45–65 Ma. Such a result gives space for interpretation of concordance or slight discordance. The latter one could be caused by episodic lead loss, fractionation, or infiltration Pb isotopes by a fluid or on micro-cracks. Thus, zircons showing a degree of concordance in the range of 90–110% in this paper are classified as concordant because of the overlap of the error ellipse with the concordia (e.g., Frei and Gerdes 2009, Jeffries et al. 2003, Linnemann et al. 2007, 2011).

Th/U ratios (Tab. 1, 2) are obtained from the LA-ICP-MS measurements of investigated zircon grains. U and Pb content and Th/U ratio were calculated relative to the GJ-1 zircon standard and are accurate to approximately 10%. Cathodoluminescence (CL)-images of zircons are produced by a Zeiss scanning electron microscope EVO 50 at the Senckenberg Naturhistorische Sammlungen Dresden.

4.2. Results

Investigated zircon grains of the Ober-Prauske Formation (sample Du1; Tab. 1) and of the Dubrau Formation (sample Du3; Tab. 2) are sub- to well rounded and have clear magmatic zoning. Complex zircon grains showing rims and cores are relatively scarce. Most zircons are clear and colourless to yellowish transparent. Brownish zircons are frequent. Metamict zircons and zircon grains that underwent ultra-high temperature and ultra-high pressure conditions could not be identified.

60 detrital zircon grains were analyzed from one sample of the red sandstone from the Ober-Prauske Formation (sample Du1). U-Th-Pb data are given in Tab. 1 and Fig. 6. Of these 60 measured grains, 54 grains are concordant (in the range of 90–110% concordant; Fig. 6).

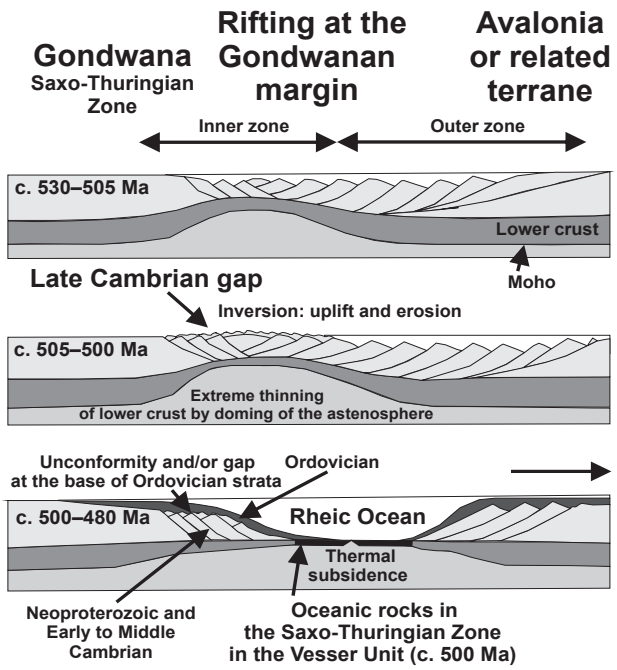

Fig. 9. Diagram illustrating the origin of the depositional gap in the Late Cambrian due to the rift setting on the periphery of the West African Craton (peri-Gondwana), eventually resulting in the formation of the Rheic Ocean and the separation of Avalonia during the Cambro-Ordovician (after Linnemann 2003).

Abb. 9. Die Entstehung der Ablagerungslücke während des späten Kambriums an der Peripherie des Westafrikanischen Kratons (peri-Gondwana), die möglicherweise in Zusammenhang mit der Öffnung des Rheic-Ozeans und der Abspaltung Avalaonias während des Oberkambriums steht (nach Linnemann 2003).

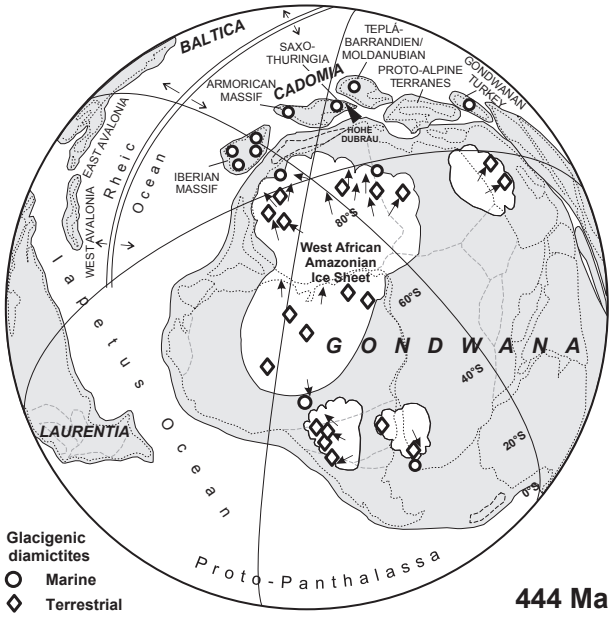

Fig. 10. Reconstruction of the palaeogeography during the Ordovician (~ 444 Ma) and the position of the Dubrau Formation (after Linnemann et al. 2011 and references therein).

Abb. 10. Paläogeographische Rekonstruktion während des Ordoviziums (~ 444 Ma) und Position der Dubrau-Formation (nach Linnemann et al. 2011 und Zitaten ebenda).

The youngest concordant grain is 542 ± 15 Ma old. The oldest zircon yields an age of 2959 ± 44 Ma. 74% of all zircons in the sample are Neoproterozoic in age, ranging from ~ 572 – 994 Ma (Fig. 6, Tab. 1). Six grains show Mesoproterozoic ages (1031 Ma, 1057 Ma, 1077 Ma, 1112 Ma, 1318 Ma, and 1515 ± Ma). 11% of all zircons in the sample are Palaeoproterozoic in age in the range of ~ 1763 – 2328 Ma (Fig. 6, Tab. 1). 4% are Archaean grains (~ 2642 – 2959 Ma). The probability plot shows distinct peaks at ~ 575 Ma, 625 Ma, 690 Ma, and ~ 775 Ma (Fig. 6). For most of the analyzed zircon grains the Th/U ratio is lower than 1.0, indicating a felsic provenance (Tab. 2). In only one case the ratio is significant higher. Therefore, this grain came from a mafic source (Tab. 1).

120 zircon detrital zircon grains were analyzed from one sample of quartzite with *Skolithos* isp. from the Dubrau Formation (sample Du3). U-Th-Pb data are shown in Tab. 2 and Fig. 7. Of these 120 measured grains, 99 grains are concordant (in the range of 90 – 110% concordant; Fig. 7). The youngest concordant grain is 532 ± 15 Ma old. The oldest zircon yields an age of 3329 ± 32 Ma. 58% of all zircons in the sample are Neoproterozoic in age, in the range of ~ 574 – 921 Ma (Fig. 7, Tab. 2). 34% of all zircons in the sample are Palaeoproterozoic in age in the range of ~ 1870 – 2471 Ma (Fig. 7, Tab. 2). 7% are Archaean grains (~ 2662 – 3329 Ma). One grain has an Early Cambrian age (532 ± 15 Ma). Mesoproterozoic zircons do not occur. The probability plot shows distinct peaks at ~ 580 Ma, 625 Ma, 700 Ma, ~ 750 Ma, ~ 1900 Ma, and 2050 Ma (Fig. 7). Small peaks scatter at ~ 2350 Ma, ~ 2900 Ma, and ~ 3200 Ma (Fig. 7). For most of the analyzed zircon grains, the Th/U ratio is lower than 1.0, indicating a felsic provenance. In only six cases the ratio is significant higher. Therefore, these grains came from a mafic source (Tab. 2).

5. Discussion and conclusion

The spot-like distribution of the red sandstones of the Ober-Prauske Formation points to a deposition of immature red siliciclastics in Cambrian time, which became mostly eroded in pre-Ordovician time. Such Cambrian red bed deposits survived only in depressions in the palaeo-landscape (Fig. 8). Main phase of erosion of the red beds occurred during an uplift in the Late Cambrian (see later in the text). Therefore, it is very likely that the Ober-Prauske Formation is Early Cambrian in age. Red sediments are typical for the Lower Cambrian in adjoining units and do not occur in the Middle Cambrian.

Due to the finding of the key fossil *Westonisca arachne* Barrande the Dubrau Formation is Tremadocian in age (Heuse & Puura 2000). The basal conglomerate of the formation overlies the Cadomian basement (Lausitz

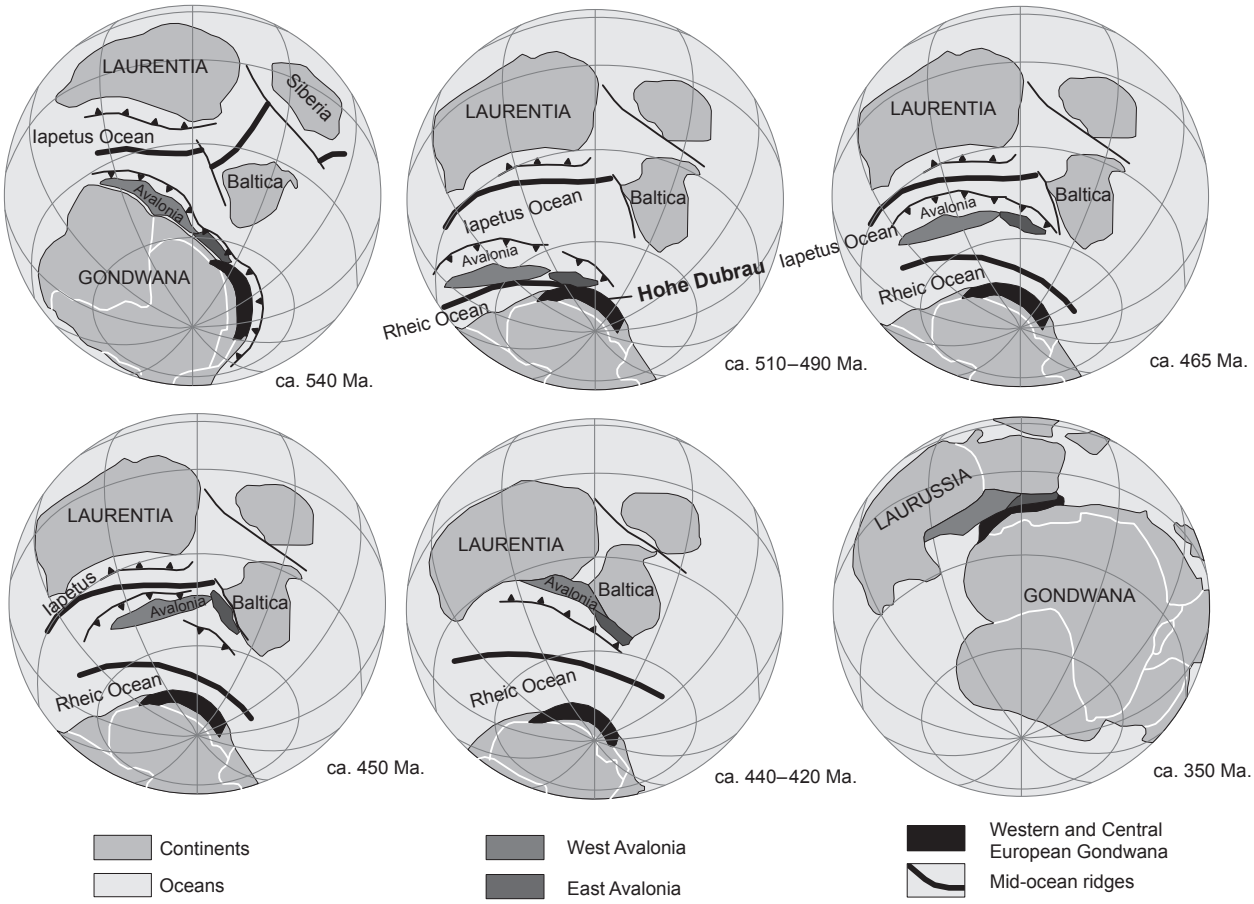

Fig. 11. Rift, drift, and collision of continents in West Gondwana from Cambrian to Carboniferous times and the formation of Pangaea – note the West African provenance of the Dubrau Formation (modified after Murphy et al. 2011).

Abb. 11. Rift, Drift und Kollision der Kontinente in West-Gondwana vom Kambrium bis zum Karbon und die Bildung Pangäas – zu beachten ist die Position der Dubrau-Formation an der Peripherie des Westafrikanischen Kratons (verändert nach Murphy et al. 2011).

Group), which was deposited around the Precambrian–Cambrian boundary at c. 545–542 Ma (Linnemann et al. 2007). The identification of the *Skolithos* and *Cruziana* ichnofacies characterize the middle part of the Dubrau Formation as deposits of the middle to lower shoreface. The depositional setting of the Dubrau Formation was a shallow marine shelf of an open sea or ocean and not a protected environment (Fig. 8). Both, the *Skolithos* and *Cruziana* ichnofacies, grade into strata characterized by frequent HCS and a lack of macrofossils, which are upper to lower offshore deposits. Thus, the whole section of the Dubrau Formation documents a trend of deepening and transgression being a part of a transgressive systems tract (TST; Fig. 8).

The lack of Middle and Upper Cambrian strata in the section may have been originated by the rift and drift-off of Avalonia or a related terrane. Rift-related doming of the astenosphere led to an inversion of the crust and as a consequence to uplift and erosion of Cambrian strata (Fig. 9; Linnemann 2003, Franz 2009, Linnemann et al. 2010). Thermal subsidence at the beginning of the Ordovician caused the new onset of deposition. One of the resulting deposits was the Dubrau Formation. The high maturity of the sedimentary rocks of the Dubrau Formation and of a lot of other Lower Ordovician sediments in the Saxo-Thuringian Zone was caused by strong chemical weathering in the source areas during the Cambrian (Linnemann et al. 2010, 2011).

On the base of the U-Pb dating of the detrital zircon grains from the Ober-Prauske and Dubrau formations a derivation of the clastic debris from the West African Craton in this paper is concluded (Fig. 10). Typical for the provenance from the West African Craton in the pattern of detrital zircon spectra is a magmatic gap in the range of c. 1.0–1.6 Ga, peaks at c. 2.0 Ga and c. 2.5 Ga, and a few Archean ages (Nance & Murphy 1994, Keppie et al. 2003, Zeh & Gerdes 2006, Linnemann et al. 2007, 2011, Drost et al. 2011). All other continents, which are principal candidates for sediment supply during Ordovician times (Baltica, Avalonia, Amazonia) show a strong portion of Mesoproterozoic zircon grains (Nance & Murphy 1994, Keppie et al. 2003, Gerdes & Zeh 2006, Linnemann et al. 2011). The six Mesoproterozoic zircon grains from the Ober-Prauske Formation point to a little sedimentary input from Amazonia, which was the neighbour of West Africa in Early Palaeozoic times. The total lack of Mesoproterozoic zircons in the Dubrau Formation completely rules out Baltica, Avalonia, and Ama-

zonia as sources for the siliciclastic sediments of this formation. Instead, the age patterns of detrital zircons from the Dubrau Formation show clearly the fingerprint of the West African Craton. Both samples (Du1, Du3) demonstrate the strong input of siliciclastic debris and zircons from the Pan-African and Cadomian basement rocks in the range of c. 532 – 994 Ma (Figs. 6, 7). Due to the overall zircon patterns in the samples Du1 and Du3, the Ober-Prauske and Dubrau formations were formed on the periphery of the West African Craton (peri-Gondwana), which is in line with most palaeobiogeographical and palaeomagnetic reconstructions and constraints from sedimentology and basin development (Robardet 2002, 2003, Linnemann et al. 2007, 2010, 2011, Drost et al. 2011). During the formation of Pangaea and the related origin of the Variscan Orogen, the peri-Gondwanan Lausitz Block, including the Ober-Prauske and Dubrau formations, was incorporated into the Central European Variscides (Fig. 11).

6. References

Brause, H. (1969): Das verdeckte Altpaläozoikum der Lausitz und seine regionale Stellung. – Abh. Dt. Akad. Wiss. Berlin, Kl. Bergbau, Hüttenw., Montangeol., **1968**: 1 – 143, Berlin.

Crimes, T.P. (1975): The production and preservation of trilobite resting and furrowing traces. – Lethaia, **8**: 35 – 48, Hoboken, New Jersey.

Drost, K.; Gerdes, A.; Jeffries, T.; Linnemann, U.; Storey, C. (2010): Provenance of Neoproterozoic and early siliciclastic rocks of the Teplá-Barrandian unit (Bohemian Massif): Evidence from U-Pb detrital zircon ages. – Gondwana Research, **19**: 213 – 231, Amsterdam.

Franz, C. (2009): Uran-Blei-Datierung detritischer Zirkone aus kambro-ordovizischen Sandsteinen der Hohen Dubrau (Lausitz-Block, Saxothuringische Zone). – 1 – 104, Dresden (unpubl. diploma thesis, TU Dresden).

Frei, D.; Gerdes, A. (2009): Precise and accurate in situ U-Pb dating of zircon with high sample throughput by automated LA-SF-ICP-MS. – Chemical Geology, **261**: 261 – 270, Amsterdam.

Frey, R.W.; Seilacher, A. (1980): Uniformity in marine invertebrate ichnology. – Lethaia, **13**: 183 – 207, Hoboken, New Jersey.

Freyer, G. (1967): Schichtung und Biostratinomie im unteren Teil des Dubrauquarzit-Komplexes. – Abh. Ber. Naturkundemus. Görlitz, **42**: 1 – 11, Görlitz.

Freyer, G.; Wiefel, H. (1991): Ein Brachiopodenfund aus der Frauenbach-Wechsellagerung des Schwarzburger Sattels. – Veröff. Naturhist. Mus. Schleusingen, **6**: 60 – 62, Schleusingen.

Gerdes, A.; Zeh, A. (2006): Combined U-Pb and Hf isotope LA-(MC-)ICP-MS analysis of detrital zircons: Comparison with SHRIMP and new constraints for the provenance and age of an Armorican metasediment in Central Germany. – Earth Planet. Sci. Lett., **249**: 47 – 61, Amsterdam.

Geinitz, H.B. (1873): Paläontologische Mittheilungen aus dem Mineralogischen Museum in Dresden. – Sitzungsber. naturwiss. Ges. Isis Dresden, 1872: 125 – 131, Dresden.

Heuse, T.; Puura, I. (2000): Biostratigraphical aspects of the Cadomian unconformity in Saxo-Thuringia. – In: Lange, J.-M.; Linnemann, U.; Thalheim, K.; Kunzmann, L.; Schneider, J.; Voigt, T. (Eds.): An International Symposium in Honour of Hanns Bruno Geinitz, Abstracts and Excursion Guide. – Schr. Staatl. Mus. Min. Geol. Dresden, **11**: 75 – 79, Dresden.

Heuse, T.; Blumenstengel, H.; Elicki, O.; Geyer, G.; Hansch, W.; Maletz, J.; Sarmiento, G.N.; Weyer, D. (2010): Biostratigraphy – the faunal province of the southern margin of the Rheic Ocean. – In: Linnemann, U.; Romer, R.L. (Eds.): Pre-Mesozoic Geology of Saxo-Thuringia – From the Cadomian Active Margin to the Variscan Orogen. – 99 – 170, Stuttgart (Schweizerbart).

Keppie, J.D.; Nance, R.D.; Murphy, J.B.; Dostal, J. (2003): Tethyan, Mediterranean, and Pacific analogues for the Neoproterozoic – Paleozoic birth and development of peri-Gondwanan terranes and their transfer to Laurentia and Laurussia. – Tectonophysics, **365**: 195 – 219, Amsterdam.

Kolíha, J. (1937): Sur le Trémadocien et sur l'Arénigien inférieur en Bohême. – Bull. Soc. Géol. France, **7**: 477 – 495, Paris.

Lee, C. (1938): Schichtenfolge und Bau des Oberlausitzer Schiefergebirges. – Geotekt. F., **2**: 1 – 55, Stuttgart.

Linnemann, U.; Buschmann, B. (1995): Die cadomische Diskordanz im Saxothuringikum (oberkambrisch – tremadocische overlap-Sequenzen). – Z. geol. Wiss., **23**: 707 – 727, Berlin.

Linnemann, U.; Gehmlich, M.; Tichomirowa, M.; Buschmann, B.; Nasdala, L.; Jonas, P.; Lützner, H.; Bombach, K. (2000): From Cadomian subduction to Early Paleozoic rifting: the evolution of Saxo-Thuringia at the margin of Gondwana in the light of single zircon geochronology and basin development (Central European Variscides, Germany). – Geol. Soc. London, Spec. Publ., **179**: 131 – 153, London.

Linnemann, U. (2003): Sedimentation und geotektonischer Rahmen der Beckenentwicklung im Saxothuringikum (Neoproterozoikum – Unterkarbon). – In: Linnemann, U. (Ed.): Das Saxothuringikum. – Geol. Sax., **48/49**: 71 – 110, Dresden.

Linnemann, U.; Gerdes, A.; Drost, K.; Buschmann, B. (2007): The continuum between Cadomian Orogenesis and opening of the Rheic Ocean: Constraints from LA-ICP-MS U-Pb zircon dating and analysis of plate-tectonic setting (Saxo-Thuringian Zone, NE Bohemian massif, Germany). – In: Linnemann, U.; Nance, D.; Kraft. P.; Zulauf, G. (Eds.): The Evolution of the Rheic Ocean: From Avalonian-Cadomian Active Margin to Alleghenian – Variscan Collision. – Geol. Soc. America, Spec. Pap., **423**: 61 – 96, Boulder, Colorado.

Linnemann, U.; Hofmann, M.; Romer, R.L.; Gerdes, A. (2010): Transitional stages between the Cadomian and Variscan Orogenies: Basin development and tectonomagmatic evolution of the southern margin of the Rheic Ocean in the Saxo-Thuringian Zone (North Gondwana shelf). – In: Linnemann, U.; Romer, R.L. (Eds.): Pre-Mesozoic Geology of Saxo-Thuringia – From the Cadomian Active Margin to the Variscan Orogen. – 59 – 98, Stuttgart (Schweizerbart).

Linnemann, U.; Ouzegane, K.; Drareni, A.; Hofmann, M.; Becker, S.; Gärtner, A.; Sagawe, A. (2011): Sands of West Gondwana: An archive of secular magmatism and plate interactions – A case study from the Cambro-Ordovician section of the Tassili Ouan Ahaggar (Algerian Sahara) using U-Pb-LA-ICP-MS detrital zircon ages. – Lithos, **123**: 188 – 203, Amsterdam.

Ludwig, K.R. (2001): Users Manual for Isoplot/Ex rev. 2.49. – Berkeley Geochron. Center Spec. Publ., **1a**: 1–56, Berkeley.

Murphy, J.B.; Cousens, B.L.; Braid, J.A.; Strachan, R.A.; Dostal, J.; Keppie, J.D.; Nance, R.D. (2011): Highly deleted oceanic lithosphere in the Rheic Ocean: Implications for Paleozoic plate reconstructions. – Lithos, **123**: 165–175, Amsterdam.

Nance, R.D.; Murphy, J.B. (1994): Contrasting basement isotopic signatures and the palinspastic restoration of peripheral orogens: Example from the Neoproterozoic Avalonian-Cadomian belt. – Geology, **22**: 617–620, Boulder, Colorado.

Pemberton, S.G.; MacEachern, J.A. (1995): The sequence stratigraphic significance of trace fossils: examples from the Cretaceous foreland basin of Alberta, Canada. AAPG Mem., **64**: 429–475, Boulder, Colorado.

Pemberton, S.G.; Spila, M.; Pulham, A.J.; Saunders, T.; MacEachern, J.A.; Robbins, D.; Sinclair, I.K. (2001): Ichnology & sedimentology of shallow to marginal marine systems – Ben Nevis & Avalon Reservoirs, Jeanne d'Arc Basin. Geological Association of Canada, Short Course Notes, Volume 15. – 1–343, St. Johns Place (Geol. Assoc. Canada).

Pietzsch, K. (1962): Geologie von Sachsen (Bezirke Dresden, Karl-Marx-Stadt und Leipzig). – 1–870, Berlin (Dt. Verl. Wiss.).

Robardet, M. (2002): Alternative approach to the Variscan Belt in southwestern Europe: Preorogenic paleobiogeographical constraints. – In: Martinez Catalan, J.R.; Hatcher, R.D.J.; Arenas, R.; Diaz Garcia, F. (Eds.): Variscan-Appalachian dynamics: The building of the late Paleozoic basement. – Geol. Soc. America, Spec. Pap., **364**: 1–15, Boulder, Colorado.

Robardet, M. (2003): The Armorica 'microplate': fact or fiction? Critical review of the concept and contradictory paleobiogeographical data. – Paleogeogr., Paleoclimatol., Paleoecol., **195**: 125–148, Amsterdam.

Seilacher, A. (2007): Trace Fossil Analysis. – 1–226, Berlin, Heidelberg, New York (Springer).

Schwarzbach, M. (1934): Das Cambrium der Oberlausitz. – Abh. Naturforsch. Ges. Görlitz, **32**: 7–54, Görlitz.

Schwarzbach, M. (1936): Oberlausitzer Schiefergebirge und Boberkatzbachgebirge – ein stratigraphisch-tektonischer Vergleich. – Abh. Naturforsch. Ges. Görlitz, **32**: 31–63, Görlitz.

Sircombe, K.N. (2004): AgeDisplay: an EXCEL workbook to evaluate and display univariate geochronological data using binned frequency histograms and probability density distributions. Comput. Geosci., **30**: 21–31, Amsterdam.

Stacey, J.S.; Kramers, J.D. (1975): Approximation of terrestrial lead isotope evolution by a two-stage model. – Earth Planet. Sci. Lett., **26**: 207–221, Amsterdam.

Wagoner, J.C. van; Mitchum, R.M.; Campion, K.M.; Rahmanian, V.D. (1990): Siliciclastic sequence stratigraphy in well logs, cores, and outcrops: Concepts for high-resolution correlation of time and facies. – AAPG Methods in Exploration Series, **7**: 1–55, Boulder, Colorado.

Appendix

Table 1. U-Th-Pb isotope data of detrital zircon grains of sample Du1: red sandstone (initial red beds), n = 54 of 60 analyzed zircon grains, Cambrian, Ober-Prauske Formation, Lausitz Block, remnants of the old quarry near Ober-Prauske, Saxo-Thuringian Zone, Germany, coordinates: 51° 15′ 28.12″ N; 14° 39′ 22.37″ E, altitude: 188 m above sea level.

Tabelle 1. U-Th-Pb-Isotopendaten der Probe Du1.

Sample Du1 Spot number	$^{207}Pb^{a}$ (cps)	U^{b} (ppm)	Pb^{b} (ppm)	Th^{b}/U	$^{206}Pb^{c}/^{238}U$	2 σ (%)	$^{207}Pb^{c}/^{235}U$	2 σ (%)	$^{207}Pb^{c}/^{206}Pb$	2 σ (%)	Rho^{d}	$^{206}Pb/^{238}U$ (Ma)	2 σ (Ma)	$^{207}Pb/^{235}U$ (Ma)	2 σ (Ma)	$^{207}Pb/^{206}Pb$ (Ma)	2 σ (Ma)	conc %
a14	6941	110	10	0.84	0.0878	2.9	0.707	4.7	0.0584	3.7	0.62	542	15	543	20	545	81	100
a43	5783	66	6	0.89	0.0924	2.9	0.76	4.3	0.0593	3.2	0.68	570	16	571	19	577	69	99
a2	20678	269	25	0.43	0.0929	2.8	0.759	3.3	0.0593	1.6	0.87	572	16	574	14	578	35	99
a49	5694	41	4	0.70	0.0941	3.6	0.784	5.5	0.0604	4.2	0.65	580	20	588	25	617	90	94
a10	4879	60	6	0.63	0.0955	2.9	0.782	4.2	0.0594	3.1	0.69	588	16	587	19	582	67	101
a17	3737	44	6	2.03	0.0963	3.5	0.794	4.8	0.05978	3.4	0.72	593	20	593	22	595	73	100
a39	4488	57	5	0.24	0.0982	3.0	0.815	4.2	0.0602	2.9	0.72	604	18	605	19	612	63	99
a27	14272	203	20	0.40	0.0993	2.9	0.83	3.3	0.0603	1.7	0.86	610	17	611	15	614	37	99
a11	2790	33	3	0.44	0.1000	3.2	0.837	5.5	0.06073	4.4	0.59	614	19	618	26	630	95	98
a64	4671	35	4	1.03	0.1002	3.5	0.835	5.1	0.0604	3.6	0.69	616	21	616	24	619	78	100
a46	7516	74	8	0.40	0.1014	3.0	0.841	3.8	0.0602	2.3	0.79	622	18	620	18	609	49	102
a20	4442	59	6	0.24	0.1017	2.9	0.845	3.8	0.0603	2.5	0.75	624	17	622	18	613	54	102
a15	4918	59	6	0.38	0.1021	2.8	0.859	4.3	0.06106	3.3	0.65	626	17	630	20	641	70	98
a38	4598	67	7	0.24	0.1020	3.2	0.861	5.0	0.0612	3.7	0.65	626	19	631	24	646	81	97
a44	5458	56	6	0.21	0.1024	3.0	0.865	4.1	0.0612	2.8	0.73	629	18	633	19	647	60	97
a13	3799	48	5	0.71	0.1030	2.9	0.87	4.3	0.0615	3.2	0.68	632	17	637	20	656	68	96
a41	5694	69	8	1.19	0.1030	2.9	0.876	3.7	0.0617	2.3	0.79	632	18	639	18	663	49	95
a21	3793	50	9	3.85	0.1040	3.5	0.883	4.7	0.06159	3.1	0.75	638	21	643	22	660	66	97
a33	7700	98	12	1.27	0.1042	3.3	0.88	4.0	0.0614	2.3	0.82	639	20	642	19	652	49	98
a36	7691	125	13	0.46	0.1057	3.1	0.897	4.1	0.0616	2.6	0.77	648	19	650	20	659	55	98
a58	4105	29	3	0.67	0.1110	3.0	0.954	4.2	0.0624	3.0	0.71	679	19	680	21	686	64	99
a66	5917	29	3	0.25	0.1118	3.1	0.955	4.2	0.0620	2.8	0.74	683	20	681	21	673	61	102
a6	15123	151	18	0.65	0.1130	2.9	0.962	3.5	0.0617	1.8	0.85	690	19	684	17	664	39	104
a30	2804	40	5	0.71	0.1129	3.6	0.97	6.0	0.0621	4.7	0.61	690	24	687	30	676	101	102
a22	3729	51	5	0.11	0.1136	3.2	0.99	4.8	0.0630	3.6	0.66	694	21	697	25	709	77	98
a47	3583	33	4	0.53	0.1148	3.0	0.987	3.6	0.0624	2.0	0.84	701	20	697	18	686	42	102
a35	7481	104	15	1.59	0.1159	2.9	1.00	3.7	0.0627	2.2	0.79	707	20	705	19	697	48	101
a7	14280	133	18	1.21	0.1168	3.3	1.02	3.7	0.0631	1.7	0.89	712	22	712	19	711	35	100
a57	3348	19	3	1.28	0.1201	3.2	1.048	4.4	0.0633	3.0	0.73	731	22	728	23	717	64	102
a59	2478	11	1	0.93	0.1208	3.2	1.067	4.5	0.0641	3.2	0.71	735	22	737	24	744	67	99

Table 1 continued.

Sample Du1 Spot number	$^{207}Pb^{a}$ (cps)	U^{b} (ppm)	Pb^{b} (ppm)	Th^{b}/U	$^{206}Pb^{c}/^{238}U$	2 σ (%)	$^{207}Pb^{c}/^{235}U$	2 σ (%)	$^{207}Pb^{c}/^{206}Pb$	2 σ (%)	Rho^{d}	$^{206}Pb/^{238}U$ (Ma)	2 σ (Ma)	$^{207}Pb/^{235}U$ (Ma)	2 σ (Ma)	$^{207}Pb/^{206}Pb$ (Ma)	2 σ (Ma)	conc %
a65	5991	25	4	1.59	0.1247	3.0	1.097	3.9	0.0638	2.6	0.76	757	21	752	21	735	54	103
a61	1697	4	1	1.01	0.1274	5.8	1.150	8.2	0.0655	5.7	0.71	773	42	777	45	789	120	98
a63	4113	20	3	0.94	0.1278	3.3	1.142	9.7	0.0648	9.1	0.35	775	24	773	54	767	191	101
a31	2567	22	3	0.97	0.1294	3.1	1.14	5.5	0.0638	4.6	0.55	784	23	772	30	736	97	107
a29	1767	17	3	1.20	0.1333	4.0	1.21	7.3	0.0656	6.1	0.55	807	31	803	41	792	128	102
a28	2442	28	4	0.28	0.1407	3.2	1.268	5.3	0.0654	4.2	0.60	848	25	832	30	787	89	108
a37	4706	35	5	0.72	0.1411	3.1	1.30	3.8	0.0669	2.1	0.83	851	25	846	22	835	44	102
a26	1176	9	1	0.51	0.1454	4.8	1.370	7.1	0.0683	5.3	0.66	875	39	876	43	878	110	100
a48	6552	36	6	0.87	0.1500	2.8	1.362	3.1	0.0659	1.4	0.89	901	24	873	19	802	30	112
a62	2888	9	2	1.30	0.1503	3.4	1.441	5.8	0.0695	4.7	0.58	903	28	906	35	915	97	99
a32	12940	109	18	0.29	0.1668	3.0	1.65	3.9	0.0715	2.5	0.78	994	28	988	25	973	50	102
a5	16606	101	17	0.11	0.1790	3.1	1.82	3.3	0.0736	1.3	0.92	1062	30	1052	22	1031	26	103
a12	10507	57	11	0.53	0.1797	2.8	1.848	3.2	0.0746	1.5	0.88	1065	28	1063	22	1057	31	101
a54	4043	16	3	0.46	0.1843	3.3	1.948	9.3	0.0767	8.7	0.35	1091	33	1098	65	1112	174	98
a34	8411	62	12	0.50	0.1854	2.9	1.925	3.6	0.07531	2.1	0.80	1097	29	1090	24	1077	43	102
a51	6445	13	4	1.05	0.2446	3.0	2.870	4.5	0.0851	3.3	0.68	1411	39	1374	34	1318	64	107
a40	15064	50	14	0.67	0.2670	2.8	3.473	3.1	0.0943	1.1	0.93	1526	39	1521	24	1515	21	101
a55	37992	49	15	0.44	0.2847	2.9	4.234	3.2	0.1079	1.2	0.92	1615	42	1681	26	1763	22	92
a60	21355	15	7	1.08	0.3783	3.4	6.297	3.8	0.1207	1.7	0.89	2068	61	2018	34	1967	31	105
a18	86461	125	54	0.68	0.3891	3.1	7.016	3.3	0.1308	1.3	0.93	2119	56	2113	30	2109	22	100
a42	10428	13	6	1.24	0.4233	2.8	7.749	3.6	0.1328	2.3	0.77	2275	54	2202	33	2135	40	107
a53	19352	13	6	0.46	0.4392	5.0	8.989	5.3	0.1485	1.7	0.95	2347	99	2337	49	2328	30	101
a24	17668	22	12	1.23	0.4422	3.2	8.304	3.7	0.13619	1.9	0.86	2361	64	2265	35	2179	33	108
a16	66592	63	35	0.94	0.4618	3.1	11.381	3.8	0.17874	2.1	0.83	2448	64	2555	36	2641	34	93
a25	6533	4	3	1.57	0.5943	6.2	17.786	6.8	0.2171	2.7	0.91	3007	151	2978	68	2959	44	102

Table 2. U-Pb-Th data of detrital zircon grains of sample Du3: white quartzite with *Skolithos* isp. (Dubrau quartzite), n = 99 of 120 analyzed zircon grains, Lower Ordovician (Tremadocian), Dubrau Formation, Monumentenberg near the village of Groß-Radisch, Lausitz Block, Saxo-Thuringian Zone, Germany, coordinates: 51° 15′27.77″ N; 14°42′27.86″ E; altitude: 280 m above sea level.

Tabelle 2. U-Th-Pb-Isotopendaten der Probe Du3.

Sample Du3 Spot number	$^{207}Pb^{a}$ (cps)	U^{b} (ppm)	Pb^{b} (ppm)	Th^{b}/U	$^{206}Pb^{c}/^{238}U$	2 σ (%)	$^{207}Pb^{c}/^{235}U$	2 σ (%)	$^{207}Pb^{c}/^{206}Pb$	2 σ (%)	Rho^{d}	$^{206}Pb/^{238}U$ (Ma)	2 σ (Ma)	$^{207}Pb/^{235}U$ (Ma)	2 σ (Ma)	$^{207}Pb/^{206}Pb$ (Ma)	2 σ (Ma)	conc %
b41	3304	64	5	0.30	0.0861	2.9	0.69	4.7	0.0580	3.7	0.62	532	15	532	20	531	82	100
b51	10900	123	11	0.49	0.0875	2.0	0.70	3.0	0.0582	2.2	0.67	541	10	540	13	539	48	100

Table 2 continued.

Sample Du3 Spot number	$^{207}Pb^{a}$ (cps)	U^{b} (ppm)	Pb^{b} (ppm)	Th^{b}/U	$^{206}Pb^{c}/^{238}U$	2 σ (%)	$^{207}Pb^{c}/^{235}U$	2 σ (%)	$^{207}Pb^{c}/^{206}Pb$	2 σ (%)	Rho^{d}	$^{206}Pb/^{238}U$ (Ma)	2 σ (Ma)	$^{207}Pb/^{235}U$ (Ma)	2 σ (Ma)	$^{207}Pb/^{206}Pb$ (Ma)	2 σ (Ma)	conc %
b13	7027	130	13	0.68	0.0930	3.3	0.76	4.1	0.0592	2.4	0.81	574	18	574	18	574	53	100
b46	2995	44	5	0.96	0.0937	2.0	0.77	4.7	0.0594	4.2	0.43	578	11	578	21	581	91	99
b20	12497	259	25	0.49	0.0946	1.7	0.77	3.7	0.0594	3.3	0.46	583	9	582	17	582	72	100
a32	5738	88	9	0.64	0.0957	3.5	0.78	5.2	0.0594	3.9	0.66	589	20	588	24	583	85	101
a16	8536	182	19	0.71	0.0967	2.6	0.799	4.3	0.05996	3.3	0.62	595	15	596	19	602	72	99
a43	2989	41	4	0.66	0.0972	3.4	0.80	5.4	0.0597	4.2	0.62	598	19	597	25	593	92	101
b50	4238	52	6	0.74	0.0990	3.1	0.82	4.5	0.0604	3.3	0.68	608	18	611	21	619	72	98
b1	5536	95	10	0.79	0.0991	2.3	0.82	3.6	0.0603	2.7	0.65	609	13	610	16	613	58	99
a31	6206	96	9	0.26	0.0996	2.5	0.82	3.6	0.0599	2.6	0.70	612	15	610	17	599	56	102
b14	6111	107	11	0.59	0.1001	3.1	0.84	4.4	0.0608	3.1	0.71	615	18	619	20	633	66	97
a7	4166	50	5	0.44	0.1004	3.8	0.84	4.3	0.0607	2.1	0.88	617	22	619	20	627	44	98
a42	1638	15	2	0.80	0.1016	2.5	0.855	7.0	0.0610	6.5	0.36	624	15	627	33	641	140	97
b49	4212	31	4	1.55	0.1018	3.1	0.85	4.7	0.0605	3.5	0.67	625	19	624	22	620	75	101
b57	19046	165	18	0.62	0.1019	2.6	0.85	3.4	0.0608	2.3	0.75	626	15	627	16	632	49	99
a35	2982	37	4	0.55	0.1023	2.3	0.86	4.1	0.0608	3.3	0.58	628	14	629	19	631	71	100
b21	10380	208	23	0.80	0.1026	2.7	0.86	3.5	0.0607	2.2	0.77	630	16	630	17	630	48	100
a27	4298	60	7	0.77	0.1037	3.1	0.87	5.2	0.0608	4.2	0.59	636	19	636	25	633	91	100
b11	3748	63	7	0.71	0.1043	3.3	0.88	4.5	0.0614	3.1	0.73	639	20	642	22	653	66	98
a18	5586	89	9	0.54	0.1050	2.6	0.881	3.8	0.0609	2.7	0.69	643	16	642	18	635	58	101
a15	5947	95	10	0.66	0.1057	2.7	0.897	3.9	0.06157	2.8	0.69	648	17	650	19	659	60	98
a22	2404	41	5	0.48	0.1065	2.8	0.90	6.0	0.0614	5.3	0.48	653	18	653	29	655	113	100
b9	17065	255	29	0.56	0.1098	3.0	0.94	3.8	0.0620	2.4	0.78	672	19	672	19	674	51	100
a2	2213	32	4	0.76	0.1101	2.7	0.928	4.9	0.0612	4.1	0.55	673	17	667	24	646	88	104
a46	3406	40	4	0.36	0.1106	2.5	0.955	4.0	0.0626	3.1	0.62	676	16	680	20	695	66	97
a55	1680	15	2	0.38	0.1132	2.4	0.982	4.4	0.0629	3.7	0.55	691	16	695	22	705	78	98
a50	5306	54	6	0.02	0.1135	3.0	0.987	8.1	0.0631	7.5	0.38	693	20	697	42	710	159	98
a47	8983	154	18	0.62	0.1146	2.5	0.997	2.8	0.0631	1.2	0.90	700	17	702	14	710	26	98
b5	6144	98	12	0.64	0.1147	3.1	0.98	5.2	0.0620	4.2	0.59	700	20	694	27	676	90	104
a8	3412	47	6	0.67	0.1148	2.4	1.002	3.9	0.0633	3.1	0.61	701	16	705	20	718	66	98
a39	7767	153	18	0.52	0.1150	3.5	0.993	6.9	0.0626	5.9	0.51	702	23	700	35	696	125	101
a30	2707	42	5	0.56	0.1152	3.6	1.01	4.5	0.0635	2.8	0.79	703	24	708	23	725	59	97
a49	3142	27	3	0.71	0.1163	3.5	1.041	5.3	0.0649	4.0	0.66	709	24	724	28	771	84	92
a10	1736	24	4	1.78	0.1166	2.8	1.008	4.2	0.0627	3.1	0.67	711	19	708	22	697	67	102
a59	1403	9	1	0.51	0.1210	5.2	1.083	7.0	0.0649	4.7	0.74	737	37	745	38	772	99	95
a53	1466	13	2	0.46	0.1212	4.7	1.082	8.9	0.0647	7.6	0.53	738	33	745	48	765	159	96
a4	2184	28	4	1.15	0.1214	2.6	1.06	4.5	0.0636	3.7	0.57	739	18	736	24	727	79	102
a5	4548	68	8	0.41	0.1228	2.6	1.08	4.0	0.0640	3.0	0.65	747	18	745	21	742	64	101

Table 2 continued.

Sample Du3 Spot number	$^{207}Pb^{a}$ (cps)	U^{b} (ppm)	Pb^{b} (ppm)	Th^{b}/U	$^{206}Pb^{c}/^{238}U$	2 σ (%)	$^{207}Pb^{c}/^{235}U$	2 σ (%)	$^{207}Pb^{c}/^{206}Pb$	2 σ (%)	Rho^{d}	$^{206}Pb/^{238}U$ (Ma)	2 σ (Ma)	$^{207}Pb/^{235}U$ (Ma)	2 σ (Ma)	$^{207}Pb/^{206}Pb$ (Ma)	2 σ (Ma)	conc %
a51	3670	34	4	0.37	0.1234	2.6	1.118	4.1	0.0657	3.2	0.63	750	18	762	22	797	68	94
b36	9830	145	19	0.65	0.1237	2.7	1.10	3.5	0.0646	2.3	0.76	752	19	754	19	762	49	99
b2	17716	278	34	0.39	0.1239	2.8	1.10	5.6	0.0644	4.8	0.51	753	20	754	30	756	101	100
a61	767	3	1	0.88	0.1241	4.6	1.084	7.0	0.0633	5.2	0.67	754	33	745	37	719	110	105
a19	7532	83	10	0.30	0.1283	2.4	1.143	4.0	0.06462	3.2	0.60	778	18	774	22	762	68	102
a63	1437	11	1	0.39	0.1284	3.1	1.156	7.3	0.0653	6.6	0.43	779	23	780	41	783	139	99
a24	779	8	1	0.81	0.1286	3.5	1.151	7.7	0.06489	6.9	0.45	780	26	778	43	771	145	101
a54	924	7	1	1.39	0.1313	3.8	1.187	7.2	0.0655	6.1	0.52	795	28	794	41	792	129	100
b15	4802	60	9	0.67	0.1317	3.1	1.20	4.6	0.0662	3.3	0.69	798	24	802	26	813	69	98
a33	3273	40	7	1.38	0.1347	2.4	1.23	5.3	0.0663	4.7	0.46	815	18	815	30	817	98	100
a40	5869	46	6	0.29	0.1356	2.8	1.224	3.4	0.0655	1.8	0.84	820	22	811	19	789	38	104
a52	947	8	1	0.89	0.1385	2.8	1.266	6.1	0.0663	5.4	0.47	836	22	831	35	815	113	103
a38	5772	38	6	1.25	0.1403	2.4	1.285	2.9	0.0664	1.5	0.85	846	19	839	17	820	32	103
a20	3878	52	7	0.48	0.1425	2.6	1.291	3.5	0.0657	2.4	0.73	859	21	842	20	797	50	108
a41	2534	32	5	0.84	0.1439	3.5	1.35	8.0	0.0680	7.2	0.43	866	28	867	48	869	149	100
a66	1118	6	1	0.66	0.1493	2.9	1.426	7.7	0.0693	7.1	0.38	897	25	900	47	908	147	99
a57	2073	13	2	0.46	0.1519	4.3	1.448	6.8	0.0691	5.3	0.63	912	36	909	42	903	109	101
a58	595	4	1	0.96	0.1536	2.9	1.486	9.9	0.0702	9.5	0.30	921	25	925	62	934	195	99
a60	6352	6	2	0.77	0.3097	2.3	4.885	4.4	0.1144	3.7	0.53	1739	36	1800	38	1870	67	93
b52	27158	47	18	0.92	0.3306	2.8	5.26	3.8	0.1154	2.5	0.75	1841	45	1863	33	1887	45	98
b60	17755	31	11	0.79	0.3318	2.6	5.23	3.5	0.1143	2.3	0.74	1847	41	1857	30	1868	42	99
a13	14186	33	14	0.96	0.3369	3.0	5.33	3.4	0.1147	1.7	0.87	1872	48	1874	30	1876	31	100
b40	6893	19	10	2.53	0.3373	5.0	5.35	5.5	0.1151	2.3	0.91	1873	81	1877	48	1881	41	100
b45	20091	47	17	0.55	0.3408	3.2	5.42	4.1	0.1154	2.6	0.78	1891	53	1889	36	1886	47	100
b35	18033	62	29	1.84	0.3414	2.2	5.52	3.3	0.1172	2.4	0.68	1894	37	1903	29	1914	43	99
b12	25012	65	29	1.67	0.3436	2.5	5.57	3.0	0.1176	1.7	0.82	1904	41	1912	26	1921	31	99
b29	48396	130	52	0.82	0.3456	2.0	5.77	2.4	0.1210	1.4	0.83	1913	34	1941	21	1972	24	97
b48	9192	14	8	2.95	0.3493	4.9	5.67	6.0	0.1177	3.5	0.82	1931	82	1926	53	1921	62	101
b30	174771	510	181	0.17	0.3517	2.1	5.87	2.5	0.1210	1.3	0.84	1943	35	1957	22	1971	24	99
b59	56797	75	26	0.08	0.3564	2.4	5.95	2.9	0.1211	1.8	0.80	1965	40	1969	26	1972	32	100
a3	7884	14	6	0.77	0.3651	2.7	5.921	3.2	0.1176	1.7	0.85	2006	48	1964	29	1920	31	104
a6	5318	9	6	3.60	0.3660	3.2	6.224	3.6	0.1233	1.6	0.89	2011	55	2008	32	2005	29	100
a36	48708	135	67	1.37	0.3687	2.3	6.214	2.7	0.1222	1.4	0.85	2023	41	2006	24	1989	25	102
b31	30690	75	31	0.70	0.3695	4.3	6.33	4.9	0.1242	2.4	0.88	2027	75	2022	44	2018	42	100
b37	17718	42	17	0.48	0.3715	2.6	6.60	3.2	0.1289	1.9	0.81	2036	45	2060	29	2083	33	98
b56	25597	32	13	0.41	0.3742	2.7	6.46	3.4	0.1251	2.0	0.80	2049	48	2040	30	2030	36	101
b7	31407	62	26	0.70	0.3769	2.8	6.51	3.0	0.1253	1.1	0.93	2062	49	2047	27	2033	20	101

Table 2 continued.

Sample Du3 Spot number	$^{207}Pb^{a}$ (cps)	U^{b} (ppm)	Pb^{b} (ppm)	Th^{b}/U	$^{206}Pb^{c}/^{238}U$	2 σ (%)	$^{207}Pb^{c}/^{235}U$	2 σ (%)	$^{207}Pb^{c}/^{206}Pb$	2 σ (%)	Rho^{d}	$^{206}Pb/^{238}U$ (Ma)	2 σ (Ma)	$^{207}Pb/^{235}U$ (Ma)	2 σ (Ma)	$^{207}Pb/^{206}Pb$ (Ma)	2 σ (Ma)	conc %
b8	43955	109	64	2.71	0.3779	2.2	6.53	2.5	0.1253	1.2	0.89	2066	40	2050	23	2034	21	102
b44	67554	109	42	0.20	0.3786	3.7	6.70	4.0	0.1283	1.5	0.92	2070	65	2072	36	2075	27	100
b16	47323	103	42	0.39	0.3857	2.4	7.04	2.9	0.1325	1.7	0.82	2103	43	2117	26	2131	30	99
a26	43729	97	45	0.80	0.3878	2.3	7.110	2.9	0.1330	1.8	0.80	2113	42	2125	26	2138	31	99
a48	17997	26	11	0.32	0.3892	2.3	6.931	3.8	0.1292	2.9	0.62	2119	42	2103	34	2087	52	102
b34	95439	244	110	0.75	0.3977	3.1	7.29	3.5	0.1330	1.6	0.89	2158	57	2148	31	2137	27	101
a14	28938	55	23	0.40	0.4012	2.6	7.23	3.1	0.1308	1.6	0.86	2175	49	2141	28	2109	27	103
b38	48233	98	46	0.76	0.4054	2.8	7.69	3.2	0.1376	1.4	0.89	2194	53	2196	29	2197	25	100
a28	15802	41	18	0.38	0.4101	2.3	7.637	3.3	0.1350	2.3	0.71	2216	44	2189	30	2165	40	102
a44	14560	17	10	1.30	0.4221	3.2	8.266	3.9	0.1420	2.1	0.83	2270	62	2261	36	2252	37	101
b33	77973	163	77	0.42	0.4345	1.6	8.76	4.0	0.1462	3.6	0.40	2326	31	2314	37	2303	62	101
b53	115086	124	61	0.49	0.4429	1.9	9.51	2.2	0.1558	1.1	0.86	2364	37	2389	20	2411	19	98
b6	254700	426	193	0.16	0.4433	2.9	9.10	3.1	0.1490	1.1	0.93	2365	57	2349	29	2334	20	101
a29	6930	22	11	0.70	0.4435	2.3	8.50	3.5	0.1390	2.6	0.67	2366	46	2286	32	2215	44	107
b58	38854	26	14	0.79	0.4578	4.4	10.19	7.6	0.1615	6.2	0.58	2430	90	2452	73	2471	104	98
b24	144828	194	101	0.27	0.4882	2.0	12.19	2.4	0.1810	1.3	0.84	2563	43	2619	23	2662	21	96
b27	193714	294	165	0.63	0.4884	2.8	11.36	3.2	0.1687	1.6	0.87	2564	59	2553	30	2545	26	101
b19	99848	114	69	0.81	0.5047	2.3	12.78	2.8	0.1836	1.6	0.81	2634	49	2664	27	2686	27	98
b32	310120	435	233	0.25	0.5060	2.9	12.50	3.2	0.1792	1.5	0.89	2639	62	2643	31	2645	25	100
b43	76744	67	43	0.50	0.5613	2.4	15.59	2.8	0.2014	1.5	0.84	2872	55	2852	27	2838	25	101
b42	113823	102	62	0.16	0.5615	2.9	15.65	3.4	0.2021	1.8	0.85	2873	67	2855	33	2843	30	101
a21	8737	6	5	1.61	0.5712	2.3	15.364	3.6	0.19508	2.8	0.64	2913	55	2838	35	2785	46	105
b25	232349	206	157	0.65	0.6303	1.5	20.91	2.0	0.2405	1.4	0.74	3151	38	3134	20	3124	22	101
a9	35989	18	13	0.28	0.6462	3.3	22.358	3.4	0.2509	0.8	0.97	3213	83	3199	33	3191	13	101
b3	45192	28	23	0.56	0.6598	3.9	23.32	4.2	0.2564	1.7	0.91	3266	100	3240	42	3224	27	101
b17	100432	83	69	0.86	0.6793	3.1	25.67	3.7	0.2740	2.1	0.83	3342	82	3334	37	3329	32	100

[a] Within-run background-corrected mean ^{207}Pb signal in counts per second

[b] U and Pb content and Th/U ratio were calculated relative to GJ-1 and are accurate to approximately 10%

[c] Corrected for background, mass bias, laser induced U-Pb fractionation and common Pb (if detectable, see analytical method) using Stacey & Kramers (1975) model Pb composition. $^{207}Pb/^{235}U$ calculated using $^{207}Pb/^{206}Pb/(^{238}U/^{206}Pb \times 1/137.88)$. Errors are propagated by quadratic addition of within-run errors (2SE) and the reproducibility of GJ-1 (2SD)

[d] Rho is the error correlation defined as $err^{206}Pb/^{238}U/err^{207}Pb/^{235}U$.